Development of hydrophobically modified polysaccharide hydrogels for use as biomaterials

March 2022

Evans Courtney Sian

Contents

List of Figures.....iv

List of Tables.....vii

Chapter 1 General introduction.....1

1-1 INTRODUCTION.....1

1-2 DISSERTATION OUTLINE.....9

1-3 REFERENCES.....10

Chapter 2 Optimized hydrophobically modified chitosan cryogels for strength and drug delivery systems.....17

2-1 INTRODUCTION.....17

2-2 MATERIALS AND METHODS.....20

2-3 RESULTS AND DISCUSSION.....25

2-4 REFERENCES.....40

Chapter 3 Fabrication of novel hydrophobically modified agarose cryogels for use as biomaterials.....45

3-1 INTRODUCTION.....45

3-2 MATERIALS AND METHODS.....48

3-3 RESULTS AND DISCUSSION.....55

3-4 REFERENCES.....63

Chapter 4 Isotherms, Kinetics and Thermodynamics of HMC and HMA Cryogels 67

4-1 INTRODUCTION 67

4-2 MATERIALS AND METHODS 68

4-3 RESULTS AND DISCUSSION 73

4-4 REFERENCES 86

Chapter 5 Conclusion 89

5-1 CONCLUSION 89

5-2 FUTURE RESEARCH 91

Acknowledgments 92

List of Figures

Figure 1: Types of polymers used in tissue engineering (17).....4

Figure 2: Crosslinking methods of hydrogels (23).....5

Figure 3: Hydrophobically modified hydrogels (11).....7

Figure 4: Physical crosslinking in HMC hydrogel (A), the molecular structure of chitosan (B), and how alkyl groups are incorporated into chitosan through reductive amination (C) (25). 19

Figure 5: FT-IR of modified and unmodified chitosan (25).....26

Figure 6: ^{1}HNMR of modified and unmodified chitosan (25). 27

Figure 7: Contact angle of HMC (25). 28

Figure 8: Mechanisms of cryogelation of the HMC aqueous solution.....30

Figure 9: XRD of modified and unmodified chitosan cryogels and chitosan powder. 32

Figure 10: Successful formation of unmodified chitosan and HMC cryogels (A), SEM images of the porous gel skeletons of the C8/7% cryogel (B), and unmodified chitosan (C) (25). . 33

Figure 11: Young's modulus of unmodified chitosan and HMC cryogels. *p < 0.05 v.s. C8/7% [n=3] (25) 34

Figure 12: A) Samples before compression and B) samples after compression. 35

Figure 13: Swelling of C12 cryogels and unmodified chitosan cryogels in PBS. 36

Figure 14: Swelling of C12 cryogels and unmodified chitosan cryogels in PBS following compression.....37

Figure 15: L929 cells after 4 hours (A) and 48 hours (B). Dotted lines show the border between C8/7% cryogel (left) and non-covered area (right) of cell culture wells (25).....38

Figure 16: The adsorption (A) and release (B) of Rhodamine-B from the unmodified chitosan, the C8/7%, and the C12/15% cryogels (25). 39

Figure 17: Chemical structure of activated agarose hydrophobically modified using Dodecylamine (4). 46

Figure 18: ^{1}H-NMR test of HMA (4) 50

Figure 19: Fabrication of unmodified agarose cryogel using Method 1. 51

Figure 20: Fabrication of unmodified and modified agarose cryogels using Method 2. 52

Figure 21: FT-IR results for HMA (4). 56

Figure 22: Unmodified agarose hydrogel prepared using Method 2 (A) HMA10 hydrogel prepared using Method 2 (B) and unmodified agarose hydrogel prepared using Method 1 (C). (D) Compression test of unmodified and modified agarose prepared using both Method 1 and Method 2 [n = 3] (4). 59

Figure 23: Cell adhesion of HMA10 at 24 hours (A) and 48 hours (B). The left side of the plate is covered with HMA10, and the right side of the plate is uncovered. [n = 3] (4). 60

Figure 24: The percentage of cell viability in cell suspension from wells containing unmodified agarose, HMA10, and control liquid (A) and the percentage of cells adhered to unmodified agarose hydrogels (Method 1) and HMA10 hydrogels (Method 2) (B) [n = 3] (4). 61

Figure 25: Adsorption (A) and release (B) of eosin-Y in HMA10 and unmodified agarose hydrogels [n = 3]. The PBS(-) was replaced at 360 and 720 min. 62

Figure 26: A) Chemical structure of rhodamine B and B) the chemical structure of eosin Y. 69

Figure 27: Extrapolated curves of Langmuir's and Freundlich's isotherms compared to the experimental equilibrium data for A) HMC at 277.15 K, B) HMC at 293.15 K, C) HMC at 310.15 K, D) HMA at 277.15 K, E) HMA at 293.15 K, and F) HMA at 310.15 K. [n = 3] 75

Figure 28: Plot of C_e/q_e vs. C_e to determine q_{max} and K_L of HMC and HMA cryogels. A) HMC at 277.15K, B) HMC at 293.15K, C) HMC at 310.15K, D) HMA at 277.15K, E) HMA at 293.15K and F) HMA at 310.15K. 77

Figure 29: Plot of Log q_e vs Log C_e to determine K_F and 1/n of HMC and HMA cryogels. A) HMC at 277.15K, B) HMC at 293.15K, C) HMC at 310.15K, D) HMA at 277.15K, E) HMA at 293.15K and F) HMA at 310.15K. 79

Figure 30: Comparison of the experimental, pseudo first, and pseudo second orders for A) HMC at 277.15 K, B) HMA at 277.15 K, C) HMC at 310.15 K and D) HMA at 310.15 K. [n=3] 85

List of Tables

Table 1: Substitution degree, alkyl chain length, and the feeding ratio of the fatty aldehydes to the amino groups in chitosan (25). 21

Table 2: Solubility, substitution degree, and contact angle of modified and unmodified agarose (4). 49

Table 3: Adsorbate concentrations of rhodamine B for HMC experiments. 71

Table 4: Adsorbate concentrations of eosin Y for HMA experiments. 71

Table 5: Langmuir's and Freundlich's parameters for HMC. 81

Table 6: Langmuir's and Freundlich's parameters for HMA 81

Table 7: Thermodynamic constants for HMC and HMA 83

Table 8: Pseudo first and second order parameters for HMC and HMA. 84

Chapter 1 *General introduction*

1-1 INTRODUCTION

Biomaterials

Biomaterials are defined as a material of synthetic or of natural origin (excluding drugs) that treats, augments, or replaces any tissue, organ, or function of the body (1,2). To do this, biomaterials need to be mechanically capable, non-toxic, have the desired functionality, the ability to be sterilized and be biocompatible (1). Examples of common biomaterials are the fillings used to fill cavities in teeth, joint replacements, and cardiovascular repairs (3). Many of these so-called first-generation biomaterials are called bioinert, which is where the materials of the biomaterials provoke limited tissue response from the surrounding tissue (4). Today, the development of biomaterials has focused on bioactive materials, which is where the biomaterial provokes a positive interaction from the surrounding tissue (for example to encourage bone growth through bonding) (4).

Biomaterials can be made from a variety of materials including metal, ceramics, glass, and polymers (2). While many bioinert biomaterials have been made using the first three, it is polymers that have had the most success at being bioactive. Largely due to the advances in synthetic methodologies used to fabricate complex functionalized polymers, polymer biomaterials are used as contact lenses, drug delivery reservoirs, and scaffolds for tissue engineering (5).

Drug delivery systems

Research into drug delivery systems (DDS) began in the early 1950s (6). The goal of DDS at that time was to develop sustainable oral and transdermal release systems and mechanisms (7). In recent years, the focus has shifted to long-term, self-regulated, and continual controlled release delivery systems, especially systems based on nanotechnology and nanoparticle (7). However, the goal of any delivery system whether it be in the past or today is to maintain a controlled release of therapeutic drugs within the bounds of a targeted biological site (6).

One of the reasons for researching alternative DDS is that many therapeutic medicines can often be as damaging to healthy tissue as they are to the diseased or abnormal tissue they are meant to target (8,9). Many mainstream delivery mechanisms (such as injections and tablets) make it difficult for the medicine they carry to reach the targeted tissue. Medicine is often required to travel through healthy tissue causing side effects and cytotoxicity before reaching the targeted tissue. On top of this, because many current delivery mechanisms are unable to monitor therapeutic responses, larger quantities of therapeutic medicine are often introduced to the system to ensure success, which in turn results in more severe side effects and cytotoxicity (9,10). A DDS that can overcome these problems is needed.

Hydrogels

Hydrogels are three-dimensional porous polymer matrices that can absorb large amounts of liquid (11). Hydrogels are known to have the potential to be highly biocompatible

and due to their high-water content, porosity, and soft consistency, they closely mimic natural living tissue (12). Because of these factors, hydrogels have a wide range of uses not only within the medical field but also for domestic use (including absorbents in disposable diapers, water beads for plants, perfume delivery, cosmetics, and environmental applications) (13). Within the medical industry, hydrogels can be used in contact lenses, tissue fillers for plastic surgery, immunotherapy, and vaccines, to hold bacterial, tissue engineering, drug delivery, and wound dressings.

Many researchers (11,13,14) attribute the modern definition of hydrogels to Witchterle and Lim who in 1960 studied hydrophilic gels and their biological uses. Since then, research into hydrogels has grown exponentially, with the number of research publications surpassing 5000 per year since 2011 (15).

Polymers

When designing a hydrogel, material selection is important. Generally, there are three classes of materials used for creating hydrogels. These are natural polymers, synthetics polymers, and combinational polymers (14,16). Figure 1 (17) shows the different types of polymers used in biomaterial fabrication (specifically tissue engineering). Naturally derived polymers have high biocompatibility with highly effective cellular adherence and infiltration but often have low mechanical properties (18,19). Synthetic polymers can be created with specific mechanical properties and tailored biodegradability but often have low biocompatibility and cell adhesion (18,20). Scientists have yet to create a synthetic polymer that mimics a natural structure, something that naturally derived materials already have.

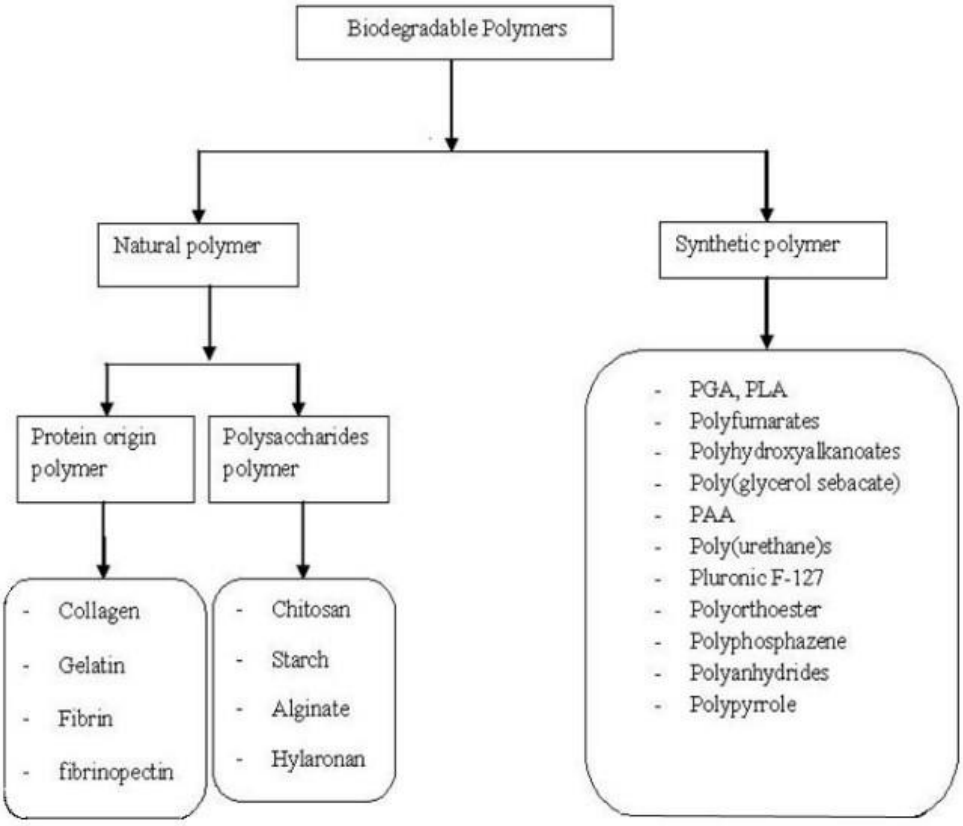

Figure 1: Types of polymers used in tissue engineering (17).

Crosslinking

Hydrogels are synthesized by crosslinking (21). Crosslinking is the process of forming reversible or covalent bonds between the monomer and the crosslinking agent (18). These bonds increase the structural and mechanical properties of the hydrogel (22). Crosslinking can be achieved through many different methods (Figure 2) that are often classified into two types – chemical crosslinking and physical crosslinking (23).

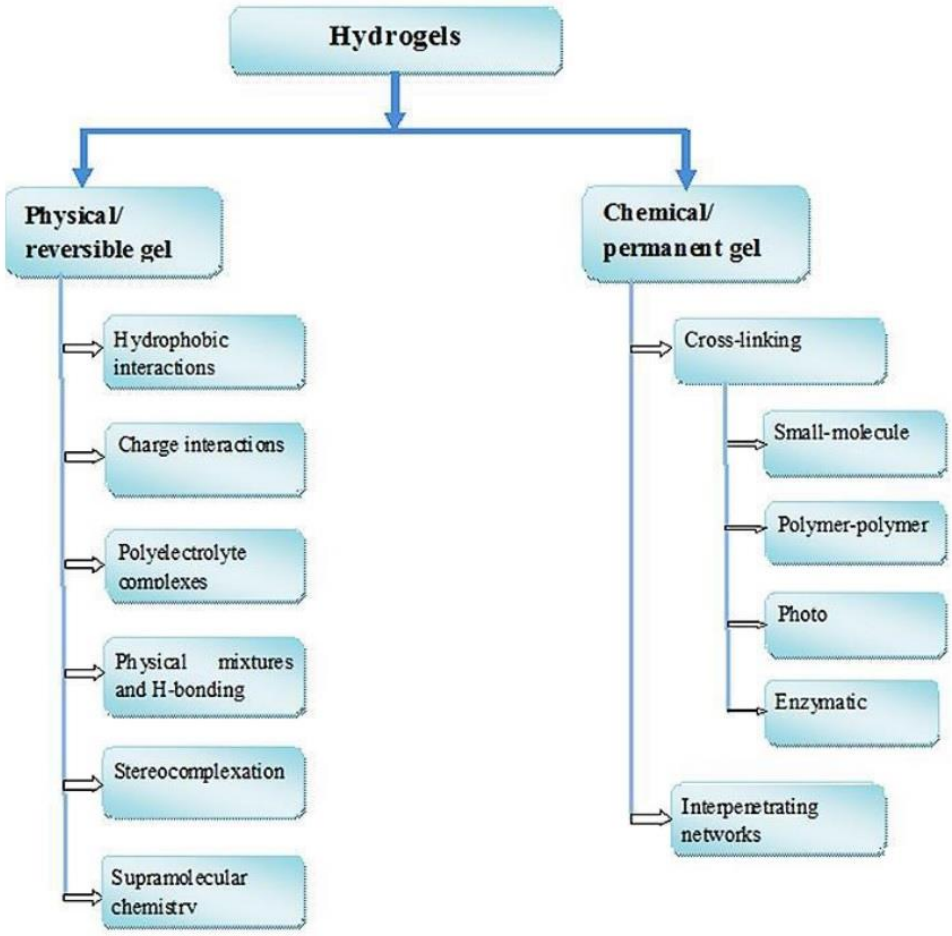

Figure 2: Crosslinking methods of hydrogels (23).

Chemical crosslinking uses chemicals to form covalent (or permanent) bonds in hydrogels (11,23). The benefits of chemical crosslinking are that the absorption and diffusion of liquids can be controlled (23). Some chemicals, such as those in the aldehyde family, can also increase the mechanical properties of the gel (14,16). However, it has often been found that even after crosslinking occurs, the crosslinking chemical remains in the solution (14,24,25). Crosslinking chemicals are often toxic and when the gel dissolves, the chemical

residue can invade surrounding cells and cause cytotoxic effects (26,27). This means that extra steps either before or after the gel is formed need to be taken to purify the gel (16,25,26). Even with purifying there is no guarantee that all the chemical residue has been removed. Attempting to purify the gels increases the cost of the gels and can increase the time taken to make the gels by weeks (25).

Physical crosslinking creates reversible or non-covalent bonds (23). Reversible gels are bonded through molecular entanglement and/or secondary forces such as ionic, hydrogen bonding, or hydrophobic interactions (11,28). Unlike chemical crosslinking (which promotes strong bonds), physical crosslinking creates fewer bonds (29) which impact the mechanical properties of the gel, producing gels with lower mechanical strength (30). Research also shows that it is difficult to control the pore size, chemical functionalization, and degradation/dissolution of gels created by physical crosslinking (31). However, the lack of chemical compounds required in crosslinking means that there is very little chance of cytotoxicity affecting the surrounding cells making physical crosslinking a popular choice.

Hydrophobic modification

The physical crosslinking method used dictates the limitations and delimitations of the hydrogel. Hydrophobically modifying polymers mainly consist of a hydrophilic backbone with hydrophobic side chains (32). Currently, hydrophobic modification is when the hydrophilic monomer is copolymerized with the hydrophobic monomer creating hydrophobic domains which act as physical crosslinking points (33). These hydrophobic

crosslinking points are then crosslinked with the hydrophilic polymer chains to form macroscopic three-dimensional gel networks (Figure 3)(11).

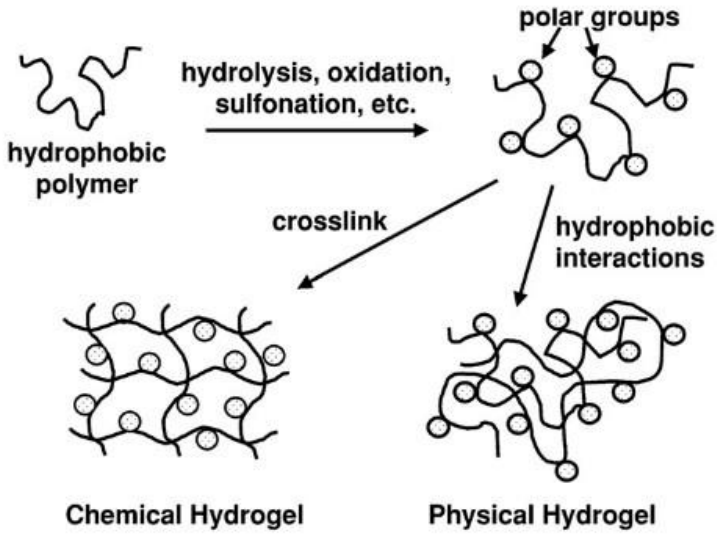

Figure 3: Hydrophobically modified hydrogels (11).

Research into hydrophobically modified polymers has been extensive over the last two decades (34). This is because hydrophobically modified polymers have been found to have increased mechanical properties (particularly strength and toughness) and the ability to selfheal compared to other physically and chemically crosslinked gels (30,33,35–37). They are also capable of allowing hydrogels (which are often extremely hydrophilic) to adsorb and release hydrophobic liquids in a controlled manner (38).

In 2010, Jiang et. al. created a hydrophobically modified hydrogel using acrylamide (AM) and octyl phenol polyoxymethylene acrylate (OP-4-AC) that exhibited excellent mechanical properties (39). Abdurrahmanoglu et. al. has also produced hydrophobically modified hydrogels using the copolymerization of acrylamide and N, N'-methylene

bis(acrylamide) (37). The strong hydrophobic association is what the authors attributed to the tough hydrogel, which had an ultimate tensile strength of approximately 80 KPa (37).

Okay, et. al. developed a dissolvable, tough, and self-healing hydrogel by copolymerizing stearyl methacrylate and dococyl acrylate with acrylamide in a micellar solution of sodium dodecyl sulfate (35). Their study found that the stearyl methacrylate hydrogels were able to self-heal at room temperature after being fractured and exhibit the original extensibility of 3600% (40).

Tuncaboylu et. al. explored the self-healing functions of a hydrophobically modified hydrogel formed by the association of sodium dodecyl sulfate (SDS) and n-alkyl (meth)acrylates (36). Their study found that hydrophobic methacrylate generates gels with more efficient self-healing than other corresponding acrylates due to limited backbone flexibility (36).

The above research focuses on hydrophobically modifying synthetic polymers through copolymerization or grafting. There is limited research on the hydrophobic modification of natural polymers. However, Inta et. al. prepared hydrophobically modified chitosan by grafting dodecenyl succinyl chains onto chitosan through phthaloylation–dodecenyl succinylation–hydrazinolysis (41). The final film showed anti-bacterial properties (41).

Jiang et. al. produced hydrophobically modified chitosan through chemical crosslinking of chitosan and palmitic anhydride in dimethyl sulfoxide (DMSO) (42). The

final hydrogels were able to adsorb and release hydrophobic drugs dependent on pH and temperature (42).

Past research into gels created by hydrophobic modification shows not only that the method can increase mechanical properties but that it can also increase the gel's reusability through higher self-healing (33,35–37). However, as seen in the examples above, mainstream research in this area continues to indicate that research is limited to copolymerization, grafting, and chemical crosslinking to hydrophobically modify synthetic polymers. Research into hydrophobically modifying natural polymers by using hydrophobic modification to physically crosslink gels is limited. To the best of our knowledge, there have been no reports where hydrogels have been formed from polysaccharide polymers by enhancing hydrophobic interactions, except for Takei et. al. who fabricated hydrophobically modified gelatin in this manner (38).

1-2 DISSERTATION OUTLINE

This study

This study proposes to advance the current knowledge of hydrophobically modified polysaccharide polymers by answering the following questions:

1. Can other polysaccharide polymers be hydrophobically modified?
2. If so, can these hydrophobically modified polysaccharide polymers be fabricated into hydrogels?
3. If successful fabrication of hydrogels occurs, what are the characteristics of the created hydrogels?

4. If successful fabrication of hydrogels occurs, what are the chemical engineering processes the gels undergo during the adsorption process of hydrophobic liquids?
5. Based on these limitations and delimitations what areas of use would the gel/gels have in the biomedical field?

Strategy of this study

The strategy of this study is as follow:

1. Perform testing to prove that the polysaccharide polymers were hydrophobically modified,
2. Identity possible fabrication methods of hydrophobically modified polysaccharide hydrogels,
3. Perform testing to identify the strength, cytotoxicity, and sorption behavior of successfully fabricated hydrogels
4. Perform testing to determine the isotherms, kinetics, and chemical engineering processes the hydrogels undergo during the adsorption of hydrophobically modified liquids.
5. From this data identify possible biomaterial uses for the fabricated hydrophobically modified polysaccharide polymers.

1-3 REFERENCES

1. **Patel, A., Mequanint, K.**: Hydrogel biomaterials; in Biomedical Engineering - Frontiers and Challenges. Edited by Fazel-Rezai R. IntechOpen, 2011 [cited 2021 Oct 7].

2. **Saha, N., Saarai, A., Roy, N., Kitano, T., Saha, P.**: Polymeric biomaterial based hydrogels for biomedical applications, J. Biomater. Nanobiotechnol., **2**, 85–90 (2011).

3. **Anjaneyulu, U., Ren, P.-G., Zhang, V.**: Ceramics for biomedical applications, Biomed. Eng. its Appl. Healthc., 229–247 (2019).

4. **Hench, L. L., Thompson, I.**: Twenty-first century challenges for biomaterials, J. R. Soc. Interface, **7**, S379–S391 (2010).

5. **Liang, Y., Li, L., Scott, R. A., Kiick, K. L.**: Polymeric biomaterials: Diverse functions enabled by advances in macromolecular chemistry, Macromolecules, **50**, 483 (2017).

6. **Li, C., Wang, J., Wang, Y., Gao, H., Wei, G., Huang, Y., Yu, H., Gan, Y., Wang, Y., Mei, L., Chen, H., Hu, H., Zhang, Z., Jin, Y.**: Recent progress in drug delivery, Acta Pharm. Sin. B, **9**, 1145–1162 (2019).

7. **Park, K.**: Controlled drug delivery systems: Past forward and future back, J. Control. Release, **190**, 3–8 (2014).

8. **Wang, X., Yang, L., Chen, Z., Shin, D. M.**: Application of nanotechnology in cancer therapy and imaging, CA. Cancer J. Clin., **58**, 97–110 (2008).

9. **Thakor, A. S., Gambhir, S. S.**: Nanooncology: The future of cancer diagnosis and therapy, CA. Cancer J. Clin., **63**, 395–418 (2013).

10. **Rawata, M., Singh, D., Saraf, S., Saraf, S.**: Nanocarriers: Promising Vehicle for Bioactive Drugs, Biol. Pharm. Bull., **29**, 1790–1798 (2006).

11. **Hoffman, A. S.**: Hydrogels for biomedical applications, Adv. Drug Deliv. Rev., **64**, 18–23 (2012).

12. **Henderson, T. M. A., Ladewig, K., Haylock, D. N., McLean, K. M., O'Connor, A. J.**: Cryogels for biomedical applications, J. Mater. Chem. B, **1**, 2682–2695 (2013).

13. **Chirani, N., Yahia, L., Gritsch, L., Motta, F. L., Chirani, S., Fare, S.**: History and applications of hydrogels, J. Biomed. Sci., **4**, 1 (2015).

14. **Priya Nagam, S., Naga Jyothi, A., Poojitha, J., Aruna, S., Rao Nadendla, R.**: A comprehensive review on hydrogels, Int. J. Curr. Pharm. Res., **8**, 19–23 (2016).

15. **Lee, S. C., Kwon, I. K., Park, K.**: Hydrogels for delivery of bioactive agents: A historical perspective, Adv. Drug Deliv. Rev., **65**, 17–20 (2013).

16. **Peppas, N. A., Hoffman, A. S.**: Hydrogels; in Biomaterials Science: An Introduction to Materials in Medicine. Academic Press, 2013 [cited 2019 May 13].

17. **Guan, L., Holy, C. E., Shoichet, M. S., Davies, J. E.**: Composite biodegradable polymer scaffold for tissue engineering., Trends Biomater. Artif. Organs, **25**, 20–29 (2011).

18. **Ma, B., Wang, X., Wu, C., Chang, J.**: Crosslinking strategies for the preparation of extracellular matrix-derived cardiovascular scaffolds., Regen. Biomater., **1**, 81–89 (2014).

19. **Anseth, K. S., Bowman, C. N., Brannon-Peppas, L.**: Mechanical properties of hydrogels and their experimental determination, Biomaterials, **17**, 1647–1657 (1996).

20. **Hassan, C. M., Peppas, N. A.**: Structure and morphology of freeze/thawed PVA hydrogels, Macromolecules, **33**, 2472–2479 (2000).

21. **Shet, R., Wong, H., Ashton, M., Dodou, K.**: Effect of crosslinking agent concentration on the properties of unmedicated hydrogels, Pharmaceutics, **7**, 305–319 (2015).

22. **Peppas, N. A., Hilt, J. Z., Khademhosseini, A., Langer, R.**: Hydrogels in biology and medicine: From molecular principles to bionanotechnology, Adv. Mater., **18**, 1345–1360 (2006).

23. **Parhi, R.**: Cross-linked hydrogel for pharmaceutical applications: A review, Adv. Pharm. Bull., **7**, 515 (2017).

24. **Peppas, N. A., Bures, P., Leobandung, W., Ichikawa, H.**: Hydrogels in pharmaceutical formulations, Eur. J. Pharm. Biopharm., **50**, 27–46 (2000).

25. **Caló, E., Khutoryanskiy, V. V**: Biomedical applications of hydrogels : A review of patents and commercial products, Eur. Polym. J., (2014).

26. **Hennink, W. E., van Nostrum, C. F.**: Novel crosslinking methods to design hydrogels, Adv. Drug Deliv. Rev., **64**, 223–236 (2012).

27. **Delgado, L. M., Bayon, Y., Pandit, A., Zeugolis, D. I.**: To cross-link or not to cross-link? Cross-linking associated foreign body response of collagen-based devices., Tissue Eng. Part B. Rev., **21**, 298–313 (2015).

28. **Ahmed, E. M.**: Hydrogel : Preparation, characterization, and applications, J. Adv.

Res., (2013).

29. **Rowland, C. R., Lennon, D. P., Caplan, A. I., Guilak, F.**: The effects of crosslinking of scaffolds engineered from cartilage ECM on the chondrogenic differentiation of MSCs., Biomaterials, **34**, 5802–5812 (2013).

30. **Tuncaboylu, D. C., Argun, A., Algi, M. P., Okay, O.**: Autonomic self-healing in covalently crosslinked hydrogels containing hydrophobic domains, Polymer (Guildf)., **54**, 6381–6388 (2013).

31. **Bhattarai, N., Gunn, J., Zhang, M.**: Chitosan-based hydrogels for controlled, localized drug delivery, Adv. Drug Deliv. Rev., **62**, 83–99 (2010).

32. **Namazi, H., Fathi, F., Dadkhah, A.**: Hydrophobically modified starch using long-chain fatty acids for preparation of nanosized starch particles, Sci. Iran., **18**, 439–445 (2011).

33. **Jiang, H., Duan, L., Ren, X., Gao, G.**: Hydrophobic association hydrogels with excellent mechanical and self-healing properties, Eur. Polym. J., **112**, 660–669 (2019).

34. **Ahearne, M., Yang, Y., Liu, K.-K.**: Mechanical characterization of hydrogels for tissue engineering applications; in Topics in Tissue Engineering. Edited by Ashammakhi N, Reis R, Chiellini F. 2008 [cited 2019 Jan 23].

35. **Tuncaboylu, D. C., Sari, M., Oppermann, W., Okay, O.**: Tough and self-healing hydrogels formed via hydrophobic interactions, Macromolecules, **44**, 4997–5005 (2011).

36. **Tuncaboylu, D. C., Argun, A., Sahin, M., Sari, M., Okay, O.**: Structure optimization of self-healing hydrogels formed via hydrophobic interactions, Polymer (Guildf)., **53**, 5513–5522 (2012).

37. **Abdurrahmanoglu, S., Can, V., Okay, O.**: Design of high-toughness polyacrylamide hydrogels by hydrophobic modification, Polymer (Guildf)., **50**, 5449–5455 (2009).

38. **Takei, T., Yoshihara, R., Danjo, S., Fukuhara, Y., Evans, C., Tomimatsu, R., Ohzuno, Y., Yoshida, M.**: Hydrophobically-modified gelatin hydrogel as a carrier for charged hydrophilic drugs and hydrophobic drugs, Int. J. Biol. Macromol., **149**, 140–147 (2020).

39. **Jiang, G., Liu, C., Liu, X., Chen, Q., Zhang, G., Yang, M., Liu, F.**: Network structure and compositional effects on tensile mechanical properties of hydrophobic association hydrogels with high mechanical strength, Polymer (Guildf)., **51**, 1507–1515 (2010).

40. **Abdurrahmanoglu, S., Cilingir, M., Okay, O.**: Dodecyl methacrylate as a crosslinker in the preparation of tough polyacrylamide hydrogels, Polymer (Guildf)., **52**, 694–699 (2011).

41. **Inta, O., Yoksan, R., Limtrakul, J.**: Hydrophobically modified chitosan: A bio-based material for antimicrobial active film, Mater. Sci. Eng. C, **42**, 569–577 (2014).

42. **Jiang, G. B., Quan, D., Liao, K., Wang, H.**: Novel polymer micelles prepared from

chitosan grafted hydrophobic palmitoyl groups for drug delivery, Mol. Pharm., **3**, 152–160 (2006).

Chapter 2 *Optimized hydrophobically modified chitosan cryogels for strength and drug delivery systems*

2-1 INTRODUCTION

When chitin becomes soluble in acidic solutions it forms chitosan. Often found in the exoskeleton of arthropods, chitin can also be found in the cell walls of fungi and yeast (1). Because chitosan is biocompatible, biodegradable, bio adhesive, promotes wound-healing, and has bacteriostatic effects it has received a great deal of interest for medical and pharmaceutical applications in recent years (2–5). Research into using chitosan as a biomaterial in wound healing, drug delivery, and tissue engineering has occurred (5–10).

Crosslinking is used to create chitosan hydrogels. Research into chemically crosslinking chitosan hydrogels is prominent (3,6,7,11,12). This is because chemically crosslinked chitosan hydrogels often have improved mechanical properties and improve the controllability of characteristics of the hydrogel (such as controlling the hydrogel to dissolve in different pH or temperatures) (12,13). Of course, the consequences of chemical crosslinking are that some chemicals can remain behind causing harmful effects, increases in cost, and production delays. (2,14).

On the flip side, physically crosslinked chitosan hydrogels do not require chemical compounds, leaving little chance of cytotoxicity affecting the surrounding tissue (2,4,14). The downside of this is that they are often less mechanically stable and not as easily controlled as hydrogels produced through chemical crosslinking (4,14).

This research explores the fabrication and characteristics of physically crosslinked chitosan hydrogels made from hydrophobically modified chitosan (HMC) (Figure 4A). Over the last two decades, research into hydrophobically modified polymers has been extensive (15). However, the hydrophobic modification of polymers is often achieved through the grafting of a hydrophilic backbone with hydrophobic side chains (16). Through hydrophobic interaction, these hydrophobic side chains can act as physical crosslinking points (17–19). The hydrophobic crosslinking points contribute to forming macroscopic three-dimensional hydrogel networks because the hydrophobic interaction is strongly exerted in an aqueous environment. Research has shown that hydrophobically modified polymers have increased mechanical properties (particularly strength and toughness) and an improved ability as carriers for hydrophobic medicines (17–21). To the best of our knowledge, our method of fabrication (by enhancing hydrophobic interaction in HMC) is novel, though some researchers have prepared HMC films for wound dressings (22) and HMC micelles for drug delivery (23,24).

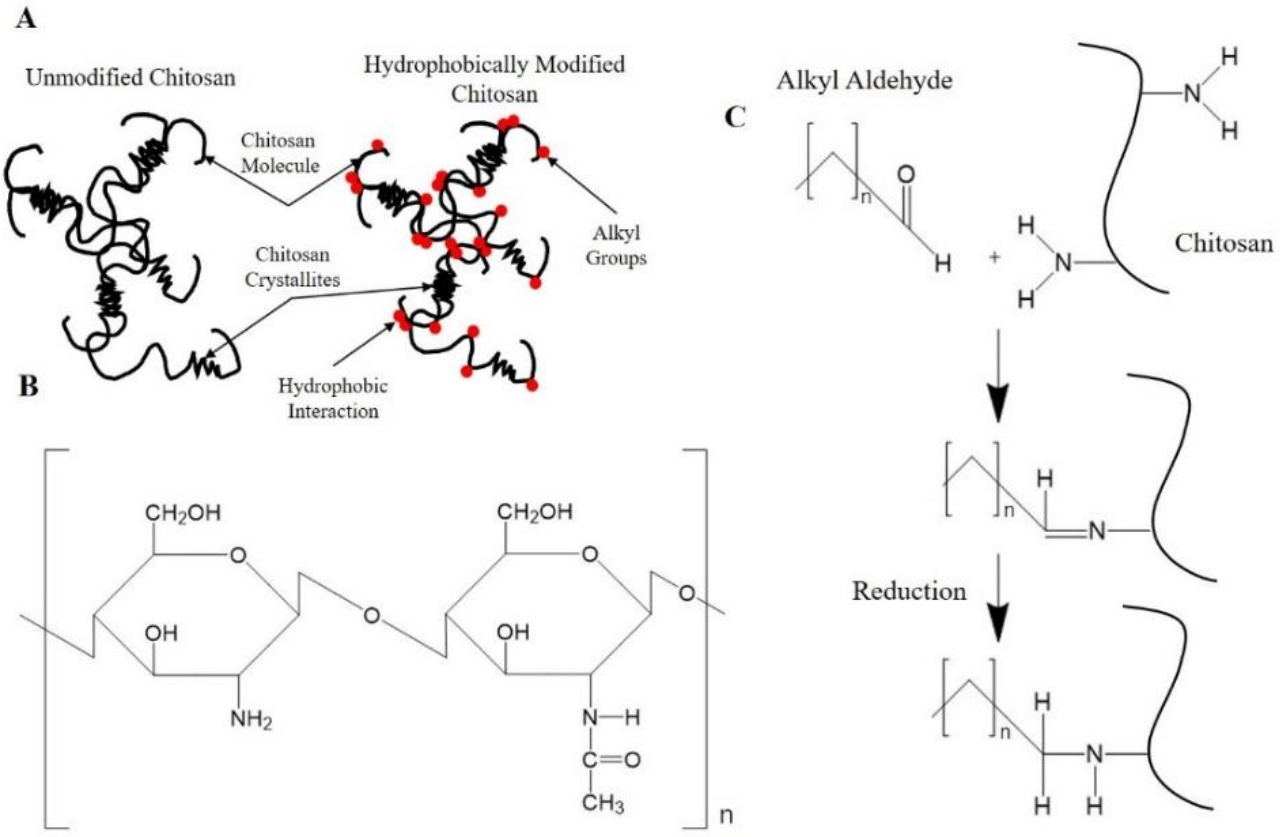

Figure 4: Physical crosslinking in HMC hydrogel (A), the molecular structure of chitosan (B) and how alkyl groups are incorporated into chitosan through reductive amination (C) (25).

By incorporating an alkyl chain into chitosan through imine bonding of the amino groups of chitosan and fatty aldehydes followed by reduction we produced hydrophobic domains and allowed for the hydrogel to be modified in two ways (Figure 4B and 4C). First, the amount of the fatty aldehyde used was varied (thereby changing the number of crosslinking points formed through hydrophobic interaction) and is known as the substitution degree. The second was the use of three different fatty aldehydes, which had different alkyl chain lengths. Through testing, this research obtained an optimized chitosan hydrogel that

has higher mechanical properties than unmodified chitosan gels and that can act as a carrier of hydrophobic medicines (25).

2-2 MATERIALS AND METHODS

Materials

Yaizu Suisankagaku Industries (Shizuoka, Japan) kindly donated Chitosan (degree of deacetylation 81%; viscosity average molecular weight 1.5x105 Da, Chitosan LL). Dodecanal, 1-Ocatanl, and Butyraldehyde were obtained from Wako Pure Chemical Industries Ltd. (Osaka, Japan). 2-Picolineborade was purchased from Junsei Chemical Co. Ltd. (Tokyo, Japan).

Synthesis of hydrophobically modified chitosan

Chitosan was dissolved in acetic acid aqueous solution at 2.0% (w/v) after which 99% ethanol was added, and the pH was increased to 5 (using sodium hydroxide (NaOH). Fatty aldehydes with different alkyl chain lengths were used to adjust the hydrophobicity of the chitosan (Table 1). 99% ethanol was used to dissolve a small amount of fatty aldehyde before being added to the chitosan solution, which was then stirred at room temperature. This allowed for the occurrence of an imine bond between the aldehyde groups in the fatty aldehyde and the amino groups in the chitosan. Afterward, 2-picolineborane was added, and the solution was stirred at room temperature in the dark to achieve reductive amination. NaOH was used to further adjust the pH of the solution to 8.0 before large amounts of 99% ethanol were added to remove any unreacted aldehyde and reductant. HMC precipitation was then freeze-dried for approximately 48 h.

Table 1: Substitution degree, alkyl chain length, and the feeding ratio of the fatty aldehydes to the amino groups in chitosan (25).

Sample	Type of fatty aldehyde	Feeding ratios for fatty aldehydes to the amino groups of chitosan (%)[b]	Substitution degree (%)	Cryogelation[a]
Unmodified Chitosan	-	-	-	+
C4/9%	C4 (Butanal)	10	9	-
C4/29%	C4 (Butanal)	25	29	-
C4/51%	C4 (Butanal)	50	51	-
C4/101%	C4 (Butanal)	100	101	-
C8/7%	C8 (Octanal)	10	7	+
C8/13%	C8 (Octanal)	25	13	+
C8/43%	C8 (Octanal)	100	43	+
C12/5%	C12 (Dodecanal)	10	5	+
C12/15%	C12 (Dodecanal)	25	15	+
C12/23%	C12 (Dodecanal)	50	23	+
C12/61%	C12 (Dodecanal)	100	61	-

[a] +: cryogel formed, -: cryogel did not form.
[b] The feeding ratio of 2-picolineborane to the amino groups in chitosan was fixed at 150%.

Fourier transform infrared spectroscopy was used to determine successful modification (Figure 5) (FT-IR, in ATR Mode, Spectrum One, Perkin Elmer, Waltham, MA, USA).

Substitution degree (SD) was calculated using hydrogen nuclear magnetic resonance (Figure 6) (^{1}H NMR, JNM-GSX-400, JEOL LTD., Tokyo, Japan). HMC was dissolved in 40% (v/v) CF_3COOD in D_2O. To obtain the SD, the number of hydrogen atoms at certain locations in the polymer structure was determined. The hydrogen atoms located in the glucosamine unit modified with alkyl aldehyde were proportional to the amount of alkyl

aldehyde bond and, therefore, showed as peaks on the graph (Figure 6). Data collected from the ^{1}H-NMR was used in the following formula to calculate the substitution degree:

$$Substitution\ degree\ (\%) = \left(\frac{\frac{I_{H-8}}{3}}{\frac{I_{H-7}}{3}} \times \frac{81}{19} \right) \times 100$$

Where $I_{H\text{-}8}$ is the intensity of the peak for the methyl protons in the alkyl chain incorporated into chitosan. $I_{H\text{-}7}$ is the peak assigned to the protons in the acetyl group in the N-acetylglucosamine unit. The numerator and denominator in the formula represent the mole of the alkyl chain incorporated into chitosan and the mole of amino groups in the unmodified chitosan.

Contact angle

The hydrophobicity of HMC was also observed by measuring the contact angle. 1% (w/w) of each HMC and unmodified chitosan were dissolved in 1% (w/w) of an acetic acid aqueous solution. The solution was then vacuum dried on a hydrophilic slide. Droplets (1 µL) of double distilled water were dropped onto a control slide (a blank slide), the dried unmodified chitosan slide, and the HMC slides and observed using a microscope. The angle between the droplet and the slide was used to calculate the contact angle.

Synthesis of cryogels

1% (w/v) of each HMC and unmodified chitosan were dissolved in HCL acid solution (0.1 M), after which, the pH was increased to 7.0 by adding a small amount of NaOH aqueous solution. Samples were placed in cylindrical molds and were then frozen at -30° C for more than 6 h before being thawed for approximately 2 h.

SEM analysis

The morphology of unmodified chitosan cryogels and HMC cryogels was evaluated using a scanning electron microscope (SEM). The cryogels were thawed and then refrozen before being freeze-dried for approximately 6 hours. The samples were then stuck to the testing plate with carbon tape and dusted with gold particles. Several different degrees of magnification were viewed to get an overall look at the gel.

XRD

We performed an x-ray diffraction (XRD) test comparing unmodified chitosan cryogels with C8/7% cryogels to determine if steric hindrance could be observed within the hydrogel structure.

Mechanical properties

Unmodified chitosan and HMC cryogel samples were frozen and thawed in cylindrical molds. Each sample was weighed and measured before being compressed on a Tensilon Universal Testing Machine. A 1kN sensor was used and samples were compressed at a rate of 0.5mm/min. Samples were compressed until 25N of applied force was observed. Data was exported to Excel where stress-strain graphs were made, and Young's Modulus was calculated. Young's Modulus was calculated between 0 and 20% strain at the first linear section of the stress-strain graph.

Swelling in PBS

To determine the swelling of the unmodified and the C12 modified cryogels, cylindrical samples of the cryogel with a diameter of 15mm were thawed. Excess free water

from the samples was blotted away before being submerged into phosphate buffered solution (PBS solution). The weight of each sample was then measured at set intervals (0 min, 30 min, 60 min, and 180 min). The swelling was calculated using the difference between the initial weight and the swelled weight.

Cellular adhesion and cytotoxicity

Cellular adhesiveness and cytotoxicity were observed using L929 fibroblast cells. L929 fibroblast cells were maintained in a cell medium that was supplemented by 10% fetal bovine solution and 0.01% (w/v) of streptomycin. Unmodified chitosan samples and C8/7% samples were smeared over half of each well in a 12-well cell culture plate. 4.0 x 10^4 cells/mL cell suspension was prepared and 0.5mL was added to each well. Cells were observed under the microscope at 4 and 48 hours after cell seeding occurred.

Absorption and release of the hydrophobic dye

Cryogels were prepared in cylindrical molds and submerged into phosphate buffer saline (PBS (pH 7.4)) containing 1.0 μM of rhodamine-B. After gently shaking the gel and solution at 4 °C and collecting liquid samples at appropriate intervals, the absorbance was measured using a UV-spectrometer at 554 nm to determine the amount of the dye adsorbed to the cryogels.

After the cryogels and rhodamine B solution had reached adsorption equilibrium, the cryogels were removed, and then they were immersed in 1mL of fresh PBS and shaken at 37 °C. PBS samples were tested using a UV- spectrometer at 554 nm to identify the amount

of rhodamine-B released. PBS was changed at 7 h and 13 h to simulate the removal of blood via the kidneys.

2-3 RESULTS AND DISCUSSION

Hydrophobically Modified Chitosan

The creation of HMC was based on our previous research performed on creating hydrophobically modified gelatin (26). There, it was discovered that the hydrophobic alkyl chain found in fatty aldehydes could be incorporated into gelatin through an imine bonding of the fatty aldehydes and the amino groups in gelatin followed by reduction (26). Subsequently, we endeavored to modify chitosan with fatty aldehydes in much the same way. By varying the alkyl chain length and substitution degree, this research obtains a chitosan hydrogel that has higher mechanical properties than unmodified chitosan gels.

Figure 5 shows the FT-IR analysis of unmodified and modified chitosan. The band at 3429 cm^{-1} can be attributed to O-H stretching overlapping N-H stretching (27) which is a regular occurrence in chitosan FT-IR analysis. Characteristic bands that display the alkyl groups were observed at approximately 2923 cm^{-1} and 2854 cm^{-1} in both the modified and unmodified chitosan samples. As the chain length of the alkyl group and the substitution degree increase, so too does this band lengthen, indicating successful incorporation of the alkyl group into chitosan.

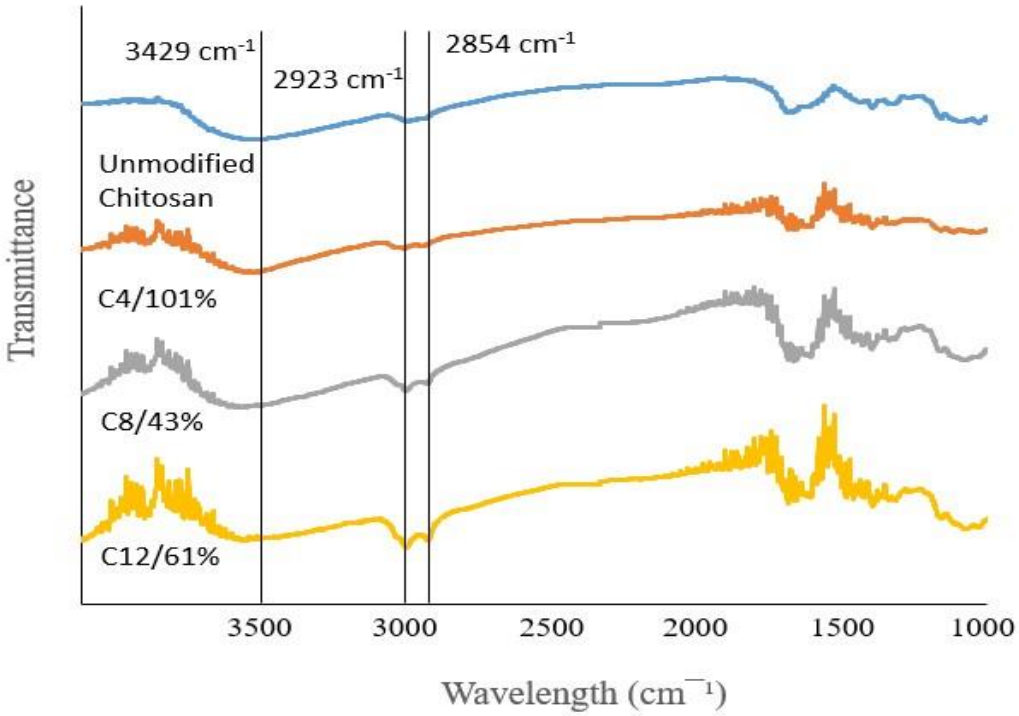

Figure 5: FT-IR of modified and unmodified chitosan (25).

From the ^{1}H NMR, the degree of substitution could be observed to be increasing with the feed ratio of aldehydes to free amino groups in the chitosan (Table 1). Table 1 shows the actual substitution degree of HMC. The substitution degree can be seen to be agreeing with the FT-IR results. Figure 6 shows a graph of the data obtained by the ^{1}H NMR. As the peak gets larger so too does the substitution degree.

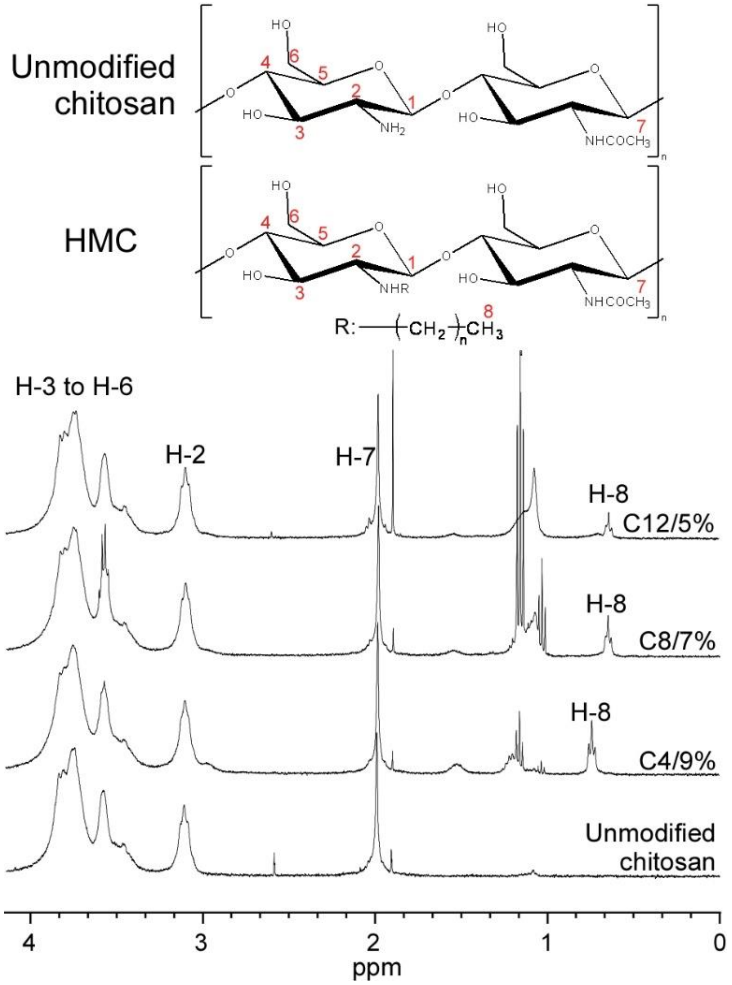

Figure 6: [1]HNMR of modified and unmodified chitosan (25).

Contact Angle

To help illustrate the hydrophobic nature of HMC, a contact angle test was performed (Figure 7). Figure 7 shows that, as expected, unmodified chitosan was more hydrophilic than water (as the contact angle for unmodified chitosan was less than the control sample). Figure 7 also shows that at 5 minutes the modified chitosan samples were more hydrophobic than water (and therefore were also more hydrophobic than unmodified chitosan) as indicated by having a larger contact angle. This shows not only the successful incorporation of the alkyl group into chitosan but also the change in nature of the chitosan from having hydrophilic properties to having hydrophobic ones.

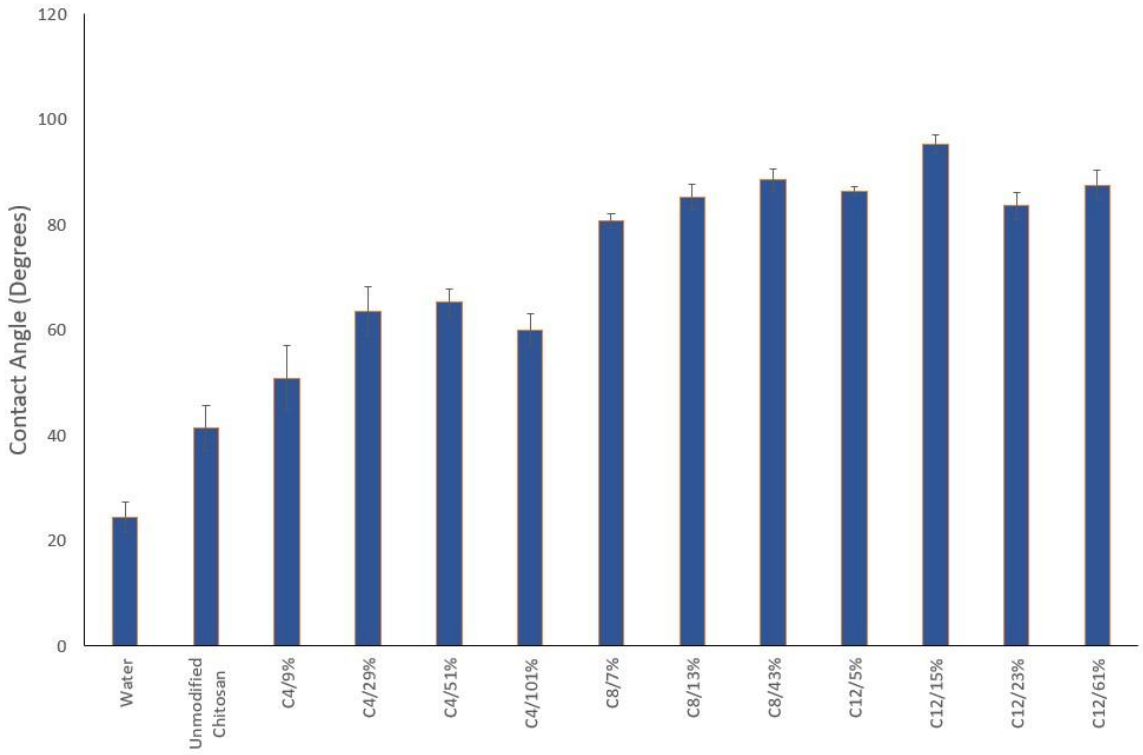

Figure 7: Contact angle of HMC (25).

Synthesis of Cryogels

Cryogelation was employed to prepare physically crosslinked HMC hydrogels. Physically crosslinked chitosan hydrogels have been prepared previously using the following cryogelation technique. In this case, first, chitosan needs to be dissolved in water. However, owing to the rigid crystalline structure, it is difficult to dissolve chitosan in water that has a neutral or alkaline pH level. Chitosan is soluble in water with an acidic pH level owing to the protonation of the amino groups in the glucosamine units. Using an acidic aqueous solution, we first dissolved chitosan before slowly increasing the pH to neutral through the gradual addition of NaOH aqueous solution. This was done slowly to limit the formation of possible chitosan precipitates. The chitosan solution was then placed in a freezer. Due to a large percentage of the chitosan solution being water, once the freezing point of water occurs, ice crystals start to form and grow. The growth of ice crystals forces the water from the solution to separate from the HMC polymer, resulting in the eventual saturation of HMC within the solution causing the formation of chitosan crystallites. These crystallites form the physical crosslinking sites of the chitosan cryogel (Figure 4A). A gel skeleton is formed if the solution has enough crystallites. After thawing, the ice water crystals melt leaving behind pores that are surrounded by the remaining HMC saturated gel skeleton. The HMC skeleton will not be affected by the free water generated through the melting of the ice crystals will because the water has a neutral pH, causing the formation of the chitosan cryogels (Figure 8).

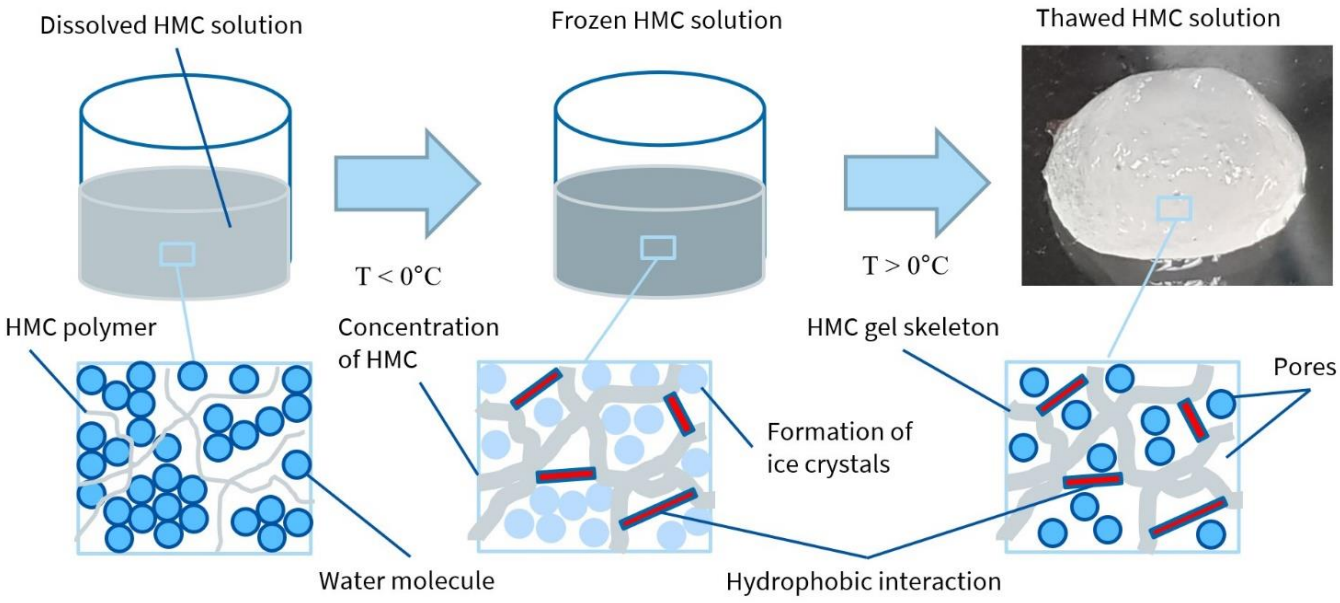

Figure 8: Mechanisms of cryogelation of the HMC aqueous solution.

Table 1 shows the successful formation of not only unmodified chitosan cryogels but also C8/7% - C8/43% and C12/15% - C12/23% cryogels. However, all cryogels created with the C4 fatty aldehyde as well as C12/61% were unable to form into successful cryogels.

From the cryogelation mechanisms described above, unmodified chitosan cryogels are established only by chitosan crystallites. Alternatively, HMC hydrogels are supported by both chitosan crystallites and hydrophobic interaction. In theory, steric hindrance could prevent the formation of chitosan crystallites due to an extremely enhanced hydrophobic interaction (for example samples with an extremely high substitution degree of fatty aldehydes). The opposite is (extremely weak hydrophobic interacting could be impeded upon by chitosan crystallites) is also true, suggesting that the balance between chitosan crystallites and hydrophobic interaction is important. In practice, testing has shown that higher

substitution degrees cause the mechanical strength of the HMC hydrogel to decrease. The formation of the C4/51%, the C4/101%, and the C12/61% cryogels could also be inhibited by extreme hydrophobic interaction. The decreased water solubility of HMC associated with enhanced hydrophobicity could be another reason that these cryogels failed to form. Although we attempted to show the water solubility of HMC to clarify it, the micelle formation of HMC in water precluded precise measurements. Furthermore, it is probable that the unsuccessful formation of the C4/9% and the C4/29% cryogels can also be attributed to the imbalance between chitosan crystallites and the hydrophobic interaction caused by shorter alkyl chain lengths (which would have caused a weaker hydrophobic interaction).

An x-ray diffraction (XRD) test was performed, comparing unmodified chitosan cryogels with C8/7% cryogels to determine if steric hindrance between the chitosan crystallites and hydrophobic interaction could be quantified. Figure 9 shows a spike on the unmodified chitosan curve at approximately $2\theta = 20$ degrees. This spike represents the chitosan crystallites. However, we were unable to identify peaks not only in the HMC12/23% cryogel but also in the unmodified chitosan cryogel. This shows that even the unmodified chitosan cryogels do not have a high enough amount of chitosan crystallites to identify on an XRD analysis. As such, we could not clarify if excessive alkyl chains prevented the formation of chitosan crystallites or not.

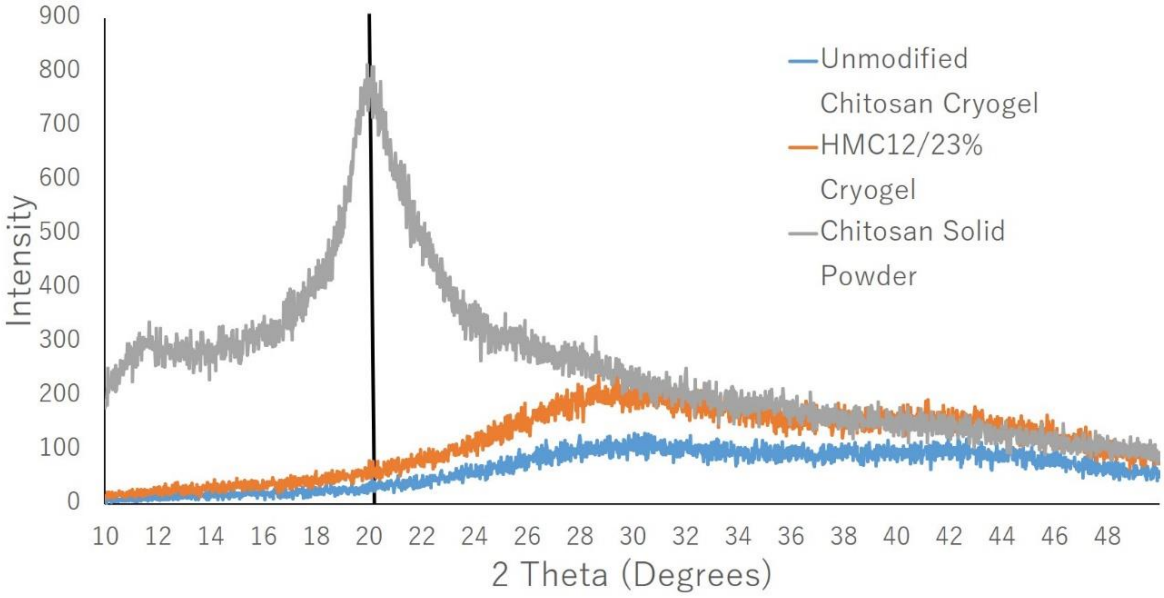

Figure 9: XRD of modified and unmodified chitosan cryogels and chitosan powder.

SEM Analysis

An SEM test was performed on modified (C8/7%) and unmodified chitosan cryogels (Figure 10B and C). At a magnification of 250, the pore size of both modified and unmodified chitosan cryogels are nearly identical and both cryogels have pores with very sheared edges.

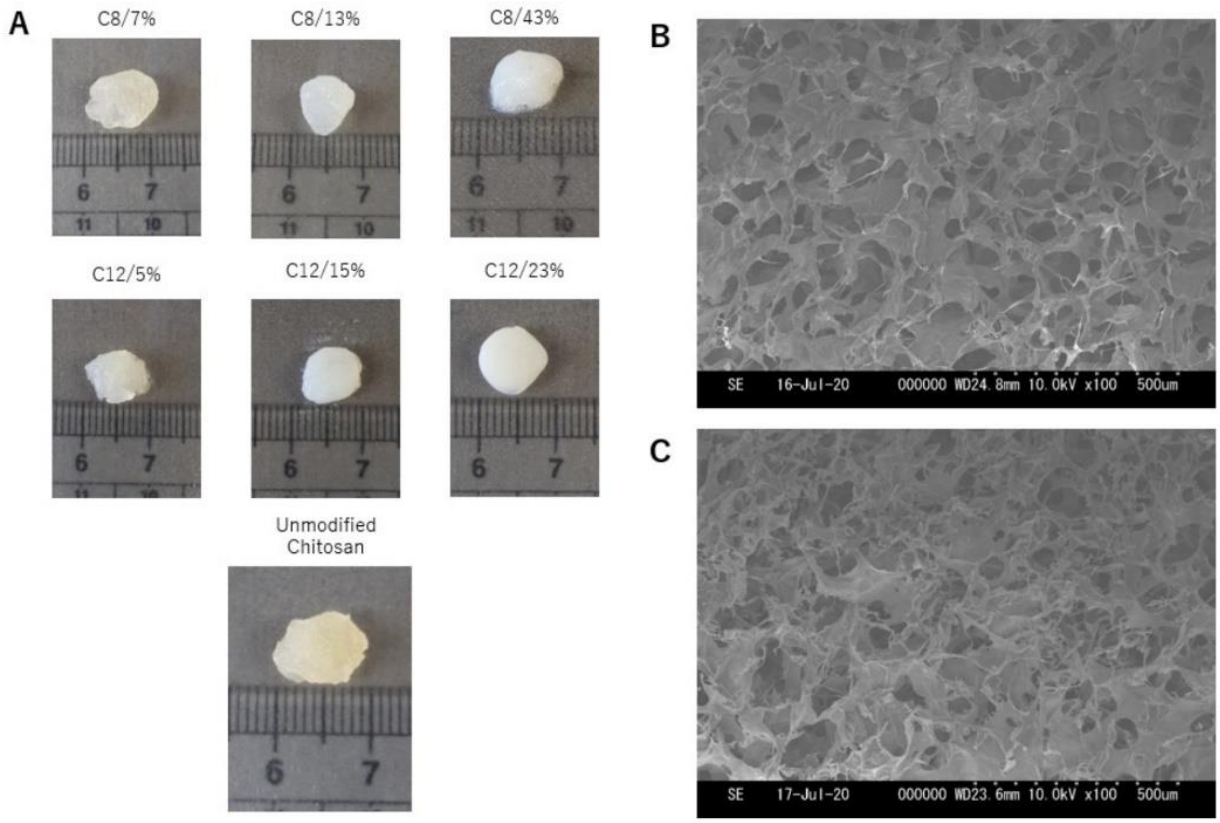

Figure 10: Successful formation of unmodified chitosan and HMC cryogels (A), SEM images of the porous gel skeletons of the C8/7% cryogel (B) and unmodified chitosan (C) (25).

Mechanical Properties

Compression testing was performed to determine the mechanical properties of both modified and unmodified chitosan. The Young's Modulus of each cryogel was found through compression testing. The Young's Modulus is used to define the stiffness of a material and can be used to identify how well a material will withstand changes in length under stress (28). Figure 11 shows the Young's Modulus for all successfully fabricated cryogels.

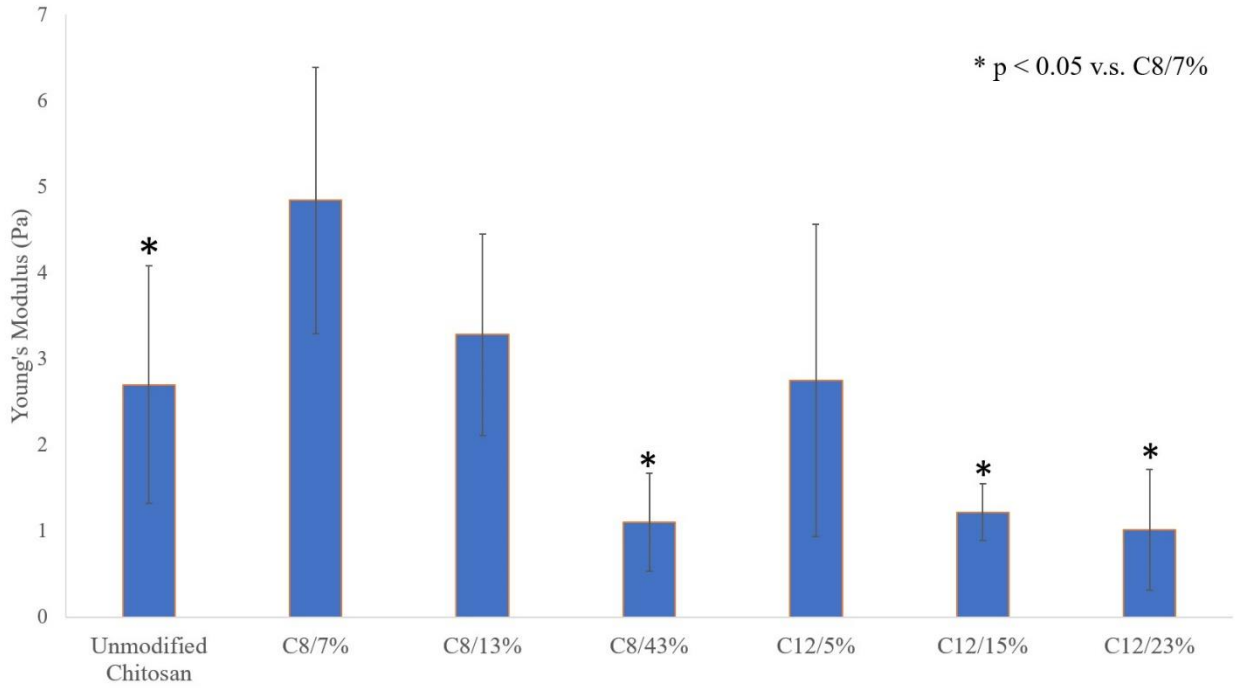

*Figure 11: Young's modulus of unmodified chitosan and HMC cryogels. *p < 0.05 v.s. C8/7% [n=3] (25)*

In Figure 11, the trend observed between all alkyl chain groups was that as the substitution degree increased (and therefore the hydrophobicity) Young's Modulus decreased. This trend is unlike previously studied hydrophobically modified polymers. The strength of hydrophobically modified gelatin (26), was observed to increase when the hydrophobicity of the polymer increased. Takei et. al. also used imide bonding between an aldehyde and the amino groups of a polysaccharide (in this case gelatin) to hydrophobically modify the polymer (26). As such, one of the major differences between the research was the polymer chosen. It could therefore be argued that the difference in polymer choice dictated the difference in compression trends.

While overall gelatin is hydrophilic it contains several amino acid groupings (proline, glycine, etc.) that are hydrophobic (29). The same cannot be said for chitosan. Chitosan is

made of D-glucosamine and N-acetyl-D-glucosamine chains, both of which are extensively hydrophilic with only minor hydrophobic side chains (1). As mentioned above, it is believed that interference between the chitosan crystallites and hydrophobic bonds is the reason for this compression trend.

In Figure 11, this theory is further proved as cryogels that had high hydrophobicity statistically had lower Young's Moduli than unmodified chitosan. Alternatively, both the C8/7% and C8/13% had statistically higher Young's Moduli than unmodified chitosan. This strength could be attributed to a stable bond between the chitosan crystallites and the hydrophobic interactions.

Figure 12 shows hydrophobically modified samples before and after compression. It was difficult to determine rupture as samples tended to flatten.

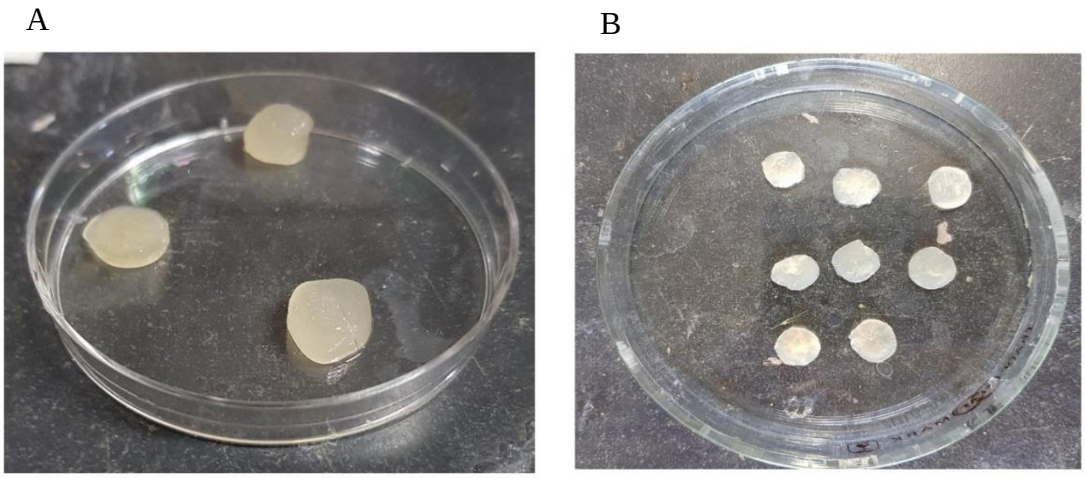

Figure 12: A) Samples before compression and B) samples after compression.

Swelling in PBS

The swelling of modified and unmodified chitosan cryogels was performed in PBS solution. There is an obvious change in mass between the unmodified chitosan and modified chitosan non-compressed samples, which appears to be dependent on the hydrophobicity of the gel (Figure 13). As the hydrophobicity of the gel increases, the amount of PBS solution absorbed into these gels is less. This supports the findings of the FT-IR which show the successful modification of the chitosan cryogels.

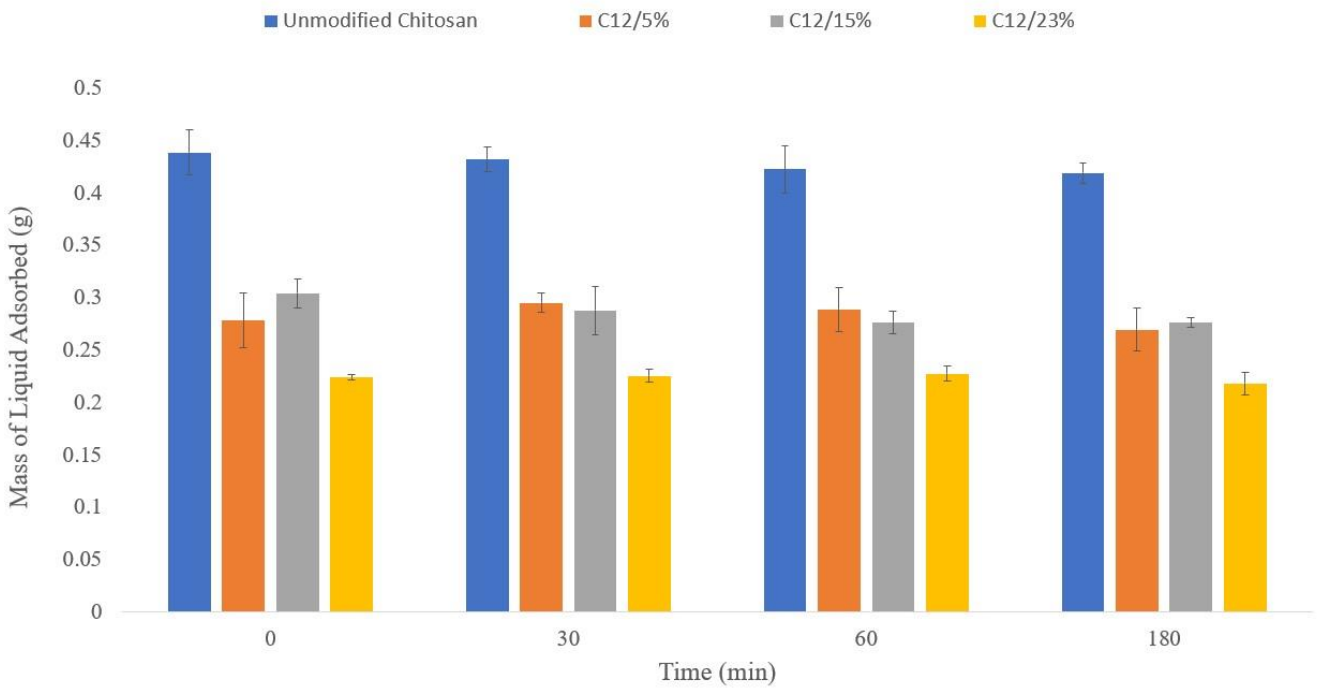

Figure 13: Swelling of C12 cryogels and unmodified chitosan cryogels in PBS.

The samples of chitosan that were used in the compression test before being used in the swelling tests (Figure 14) showed that the weight at the equilibrium point of the compressed samples (which occurred at approximately 30 minutes) did not reach as high as the samples that were not compressed. The modified chitosan compressed samples reached approximately two-thirds of the non-compressed weight and as such, it can be speculated, that there was either minimal damage from the compression testing, or the gel can repair itself to a certain degree. Previous research agreed that hydrophobically modifying cryogels helps to increase their ability to self-repair (17,19,20).

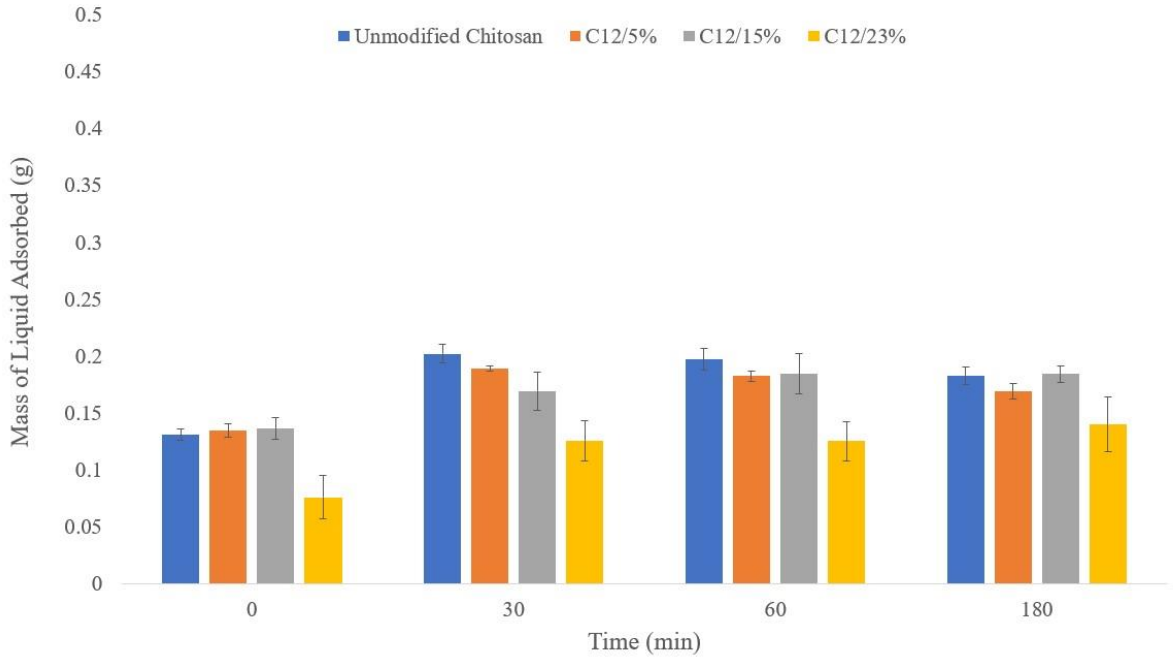

Figure 14: Swelling of C12 cryogels and unmodified chitosan cryogels in PBS following compression.

Cell Adhesion and Cytotoxicity

The cell adhesiveness test was performed on the C8/7% and the unmodified chitosan cryogels. It showed that unless the cryogel was very thin, cells would not adhere to it. However, it did show that the cytotoxicity of the gel is low as cells proliferated around the gel over the 48 hours testing period. Both observations can be seen in Figure 15.

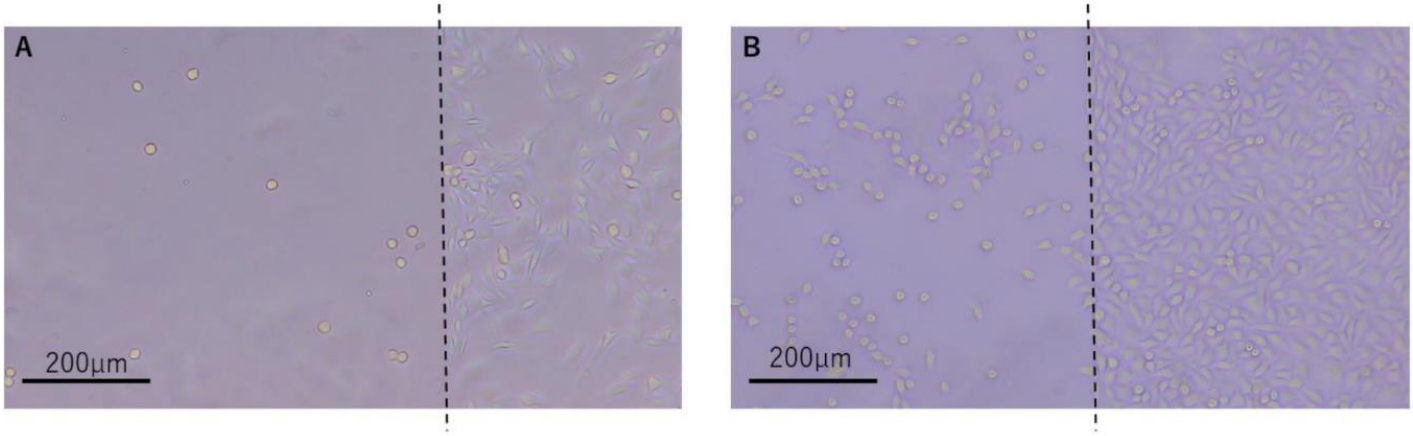

Figure 15: L929 cells after 4 hours (A) and 48 hours (B). Dotted lines show the border between C8/7% cryogel (left) and non-covered area (right) of cell culture wells (25).

Adsorption and Diffusion

Because of their enhanced hydrophobicity, it was expected that hydrophobic medicines could be adsorbed to HMC cryogels. It was also probable that, also due to their enhanced hydrophobicity, HMC cryogels would be able to gradually release hydrophobic drugs through diffusion in vivo to satisfy the adsorption equilibrium. We examined the potential of HMC cryogels as carriers of hydrophobic medicines using rhodamine-B (octanol-water partition coefficient (low Pow): 1.94) as a model for hydrophobic medicine.

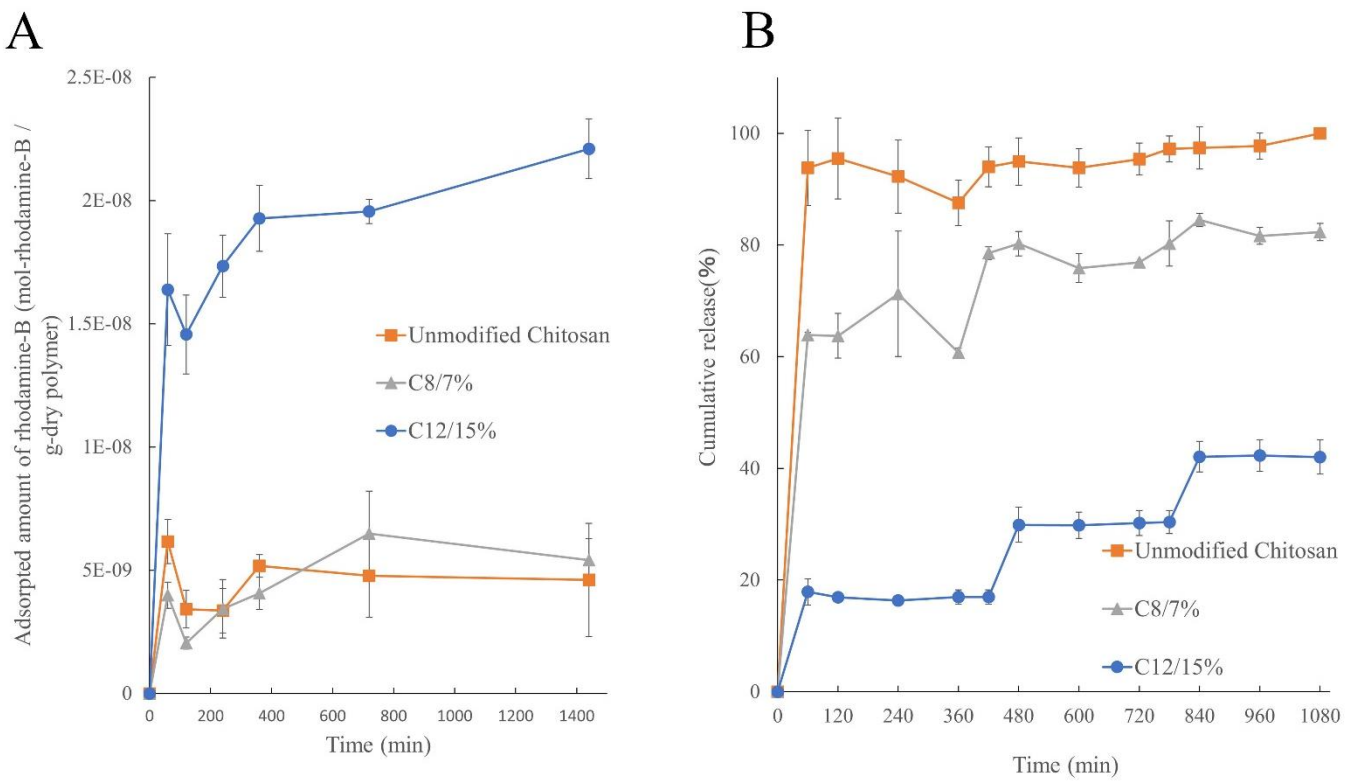

Figure 16: The adsorption (A) and release (B) of Rhodamine-B from the unmodified chitosan, the C8/7% and the C12/15% cryogels (25).

Figure 16 shows the results of the adsorption and the release behavior of rhodamine-B. The graph shows that the adsorption of rhodamine-B to unmodified chitosan and C8/7% chitosan was similar and quite low whereas the adsorption of the C12/15% cryogel was much higher.

The release test was performed in PBS. The PBS was exchanged for fresh PBS at 420 and 780 minutes to simulate the removal of the hydrophobic drug by the kidneys in vivo (26). From the unmodified chitosan and the C8/7% cryogels, rhodamine-B was released in one burst. However, the C12/15% cryogel released the rhodamine-B in a step-like pattern after every exchange of PBS. This would be owing to the strong hydrophobic interaction between

the dye and the C12/15% cryogel which causes equilibrium between the rhodamine B in the cryogel and rhodamine B in the PBS solution to be achieved quickly. Once equilibrium is reached, the driving force causing the cryogel to release rhodamine B plateaus until new PBS is added.

These results show that the C12/15% cryogel has high potential as a carrier of hydrophobic medicines.

2-4 REFERENCES

1. **Rinaudo, M.**: Chitin and chitosan: Properties and applications, Prog. Polym. Sci., **31**, 603–632 (2006).

2. **Berger, J., Reist, M., Mayer, J. M., Felt, O., Peppas, N. A., Gurny, R.**: Structure and interactions in covalently and ionically crosslinked chitosan hydrogels for biomedical applications, Eur. J. Pharm. Biopharm., **57**, 19–34 (2004).

3. **Takei, T., Nakahara, H., Ijima, H., Kawakami, K.**: Synthesis of a chitosan derivative soluble at neutral pH and gellable by freeze–thawing, and its application in wound care, Acta Biomater., **8**, 686–693 (2012).

4. **Bhattarai, N., Gunn, J., Zhang, M.**: Chitosan-based hydrogels for controlled, localized drug delivery, Adv. Drug Deliv. Rev., **62**, 83–99 (2010).

5. **Jayakumar, R., Prabaharan, M., Sudheesh Kumar, P. T., Nair, S. V., Tamura, H.**: Biomaterials based on chitin and chitosan in wound dressing applications, Biotechnol. Adv., **29**, 322–337 (2011).

6. **Azab, A. K., Orkin, B., Doviner, V., Nissan, A., Klein, M., Srebnik, M., Rubinstein, A.**: Crosslinked chitosan implants as potential degradable devices for brachytherapy: In vitro and in vivo analysis, J. Control. Release, **111**, 281–289 (2006).

7. **Takei, T., Nakahara, H., Tanaka, S., Nishimata, H., Yoshida, M., Kawakami, K.**: Effect of chitosan-gluconic acid conjugate/poly(vinyl alcohol) cryogels as wound dressing on partial-thickness wounds in diabetic rats, J. Mater. Sci. Mater. Med., **24**, 2479–2487 (2013).

8. **Sjoholm, K. H., Cooney, M., Minteer, S. D.**: Effects of degree of deacetylation on enzyme immobilization in hydrophobically modified chitosan, Carbohydr. Polym., **77**, 420–424 (2009).

9. **Ji, C., Annabi, N., Khademhosseini, A., Dehghani, F.**: Fabrication of porous chitosan scaffolds for soft tissue engineering using dense gas CO2, Acta Biomater., **7**, 1653–1664 (2011).

10. **Francis Suh, J.-K., Matthew, H. W. .**: Application of chitosan-based polysaccharide biomaterials in cartilage tissue engineering: a review, Biomaterials, **21**, 2589–2598 (2000).

11. **Gupta, A., Bhat, S., Jagdale, P. R., Chaudhari, B. P., Lidgren, L., Gupta, K. C., Kumar, A.**: Evaluation of three-dimensional chitosan-agarose-gelatin cryogel scaffold for the repair of subchondral cartilage defects: an in vivo study in a rabbit model., Tissue Eng. Part A, **20**, 3101–3111 (2014).

12. **Bhat, S., Tripathi, A., Kumar, A.**: Supermacroprous chitosan-agarose-gelatin cryogels: in vitro characterization and in vivo assessment for cartilage tissue engineering., J. R. Soc. Interface, **8**, 540–554 (2011).

13. **Giri, T. K., Thakur, A., Alexander, A., Ajazuddin, Badwaik, H., Tripathi, D. K.**: Modified chitosan hydrogels as drug delivery and tissue engineering systems: Present status and applications, Acta Pharm. Sin. B, **2**, 439–449 (2012).

14. **Ahmadi, F., Oveisi, Z., Samani, M., Amoozgar, Z.**: Chitosan based hydrogels: Characteristics and pharmaceutical applications, Research in Pharmaceutical Sciences,**10**, 1–16 (2015).

15. **Ahearne, M., Yang, Y., Liu, K.-K.**: Mechanical characterisation of hydrogels for tissue engineering applications; in Topics in Tissue Engineering. Edited by Ashammakhi N, Reis R, Chiellini F. 2008 [cited 2019 Jan 23].

16. **Namazi, H., Fathi, F., Dadkhah, A.**: Hydrophobically modified starch using long-chain fatty acids for preparation of nanosized starch particles, Sci. Iran., **18**, 439–445 (2011).

17. **Jiang, H., Duan, L., Ren, X., Gao, G.**: Hydrophobic association hydrogels with excellent mechanical and self-healing properties, Eur. Polym. J., **112**, 660–669 (2019).

18. **Tuncaboylu, D. C., Argun, A., Algi, M. P., Okay, O.**: Autonomic self-healing in covalently crosslinked hydrogels containing hydrophobic domains, Polymer (Guildf)., **54**, 6381–6388 (2013).

19. **Tuncaboylu, D. C., Sari, M., Oppermann, W., Okay, O.**: Tough and self-healing hydrogels formed via hydrophobic interactions, Macromolecules, **44**, 4997–5005 (2011).

20. **Tuncaboylu, D. C., Argun, A., Sahin, M., Sari, M., Okay, O.**: Structure optimization of self-healing hydrogels formed via hydrophobic interactions, Polymer (Guildf)., **53**, 5513–5522 (2012).

21. **Abdurrahmanoglu, S., Can, V., Okay, O.**: Design of high-toughness polyacrylamide hydrogels by hydrophobic modification, Polymer (Guildf)., **50**, 5449–5455 (2009).

22. **Inta, O., Yoksan, R., Limtrakul, J.**: Hydrophobically modified chitosan: A bio-based material for antimicrobial active film, Mater. Sci. Eng. C, **42**, 569–577 (2014).

23. **Wang, X. H., Tian, Q., Wang, W., Zhang, C. N., Wang, P., Yuan, Z.**: In vitro evaluation of polymeric micelles based on hydrophobically-modified sulfated chitosan as a carrier of doxorubicin, J. Mater. Sci. Mater. Med., **23**, 1663–1674 (2012).

24. **Jiang, G. B., Quan, D., Liao, K., Wang, H.**: Novel polymer micelles prepared from chitosan grafted hydrophobic palmitoyl groups for drug delivery, Mol. Pharm., **3**, 152–160 (2006).

25. **Evans, C., Morimitsu, Y., Hisadome, T., Inomoto, F., Yoshida, M., Takei, T.**: Optimized hydrophobically modified chitosan cryogels for strength and drug delivery systems, J. Biosci. Bioeng., **132**, 81–87 (2021).

26. **Takei, T., Yoshihara, R., Danjo, S., Fukuhara, Y., Evans, C., Tomimatsu, R., Ohzuno, Y., Yoshida, M.**: Hydrophobically-modified gelatin hydrogel as a carrier for charged hydrophilic drugs and hydrophobic drugs, Int. J. Biol. Macromol., **149**, 140–147 (2020).

27. **Kumirska, J., Czerwicka, M., Kaczyński, Z., Bychowska, A., Brzozowski, K., Thöming, J., Stepnowski, P.**: Application of spectroscopic methods for structural analysis of chitin and chitosan., Mar. Drugs, **8**, 1567–1636 (2010).

28. **Hinkley, J. A., Morgret, L. D., Gehrke, S. H.**: Tensile properties of two responsive hydrogels, Polymer (Guildf)., **45**, 8837–8843 (2004).

29. **Hafidz, R. N. R. M., Yaakob, C. M., Amin, I., Noorfaizan, A.**: Chemical and functional properties of bovine and porcine skin gelatin, Int. Food Res. J., **18**, 787–791 (2011).

Chapter 3 *Fabrication of novel hydrophobically modified agarose cryogels for use as biomaterials*

3-1 INTRODUCTION

Agarose is a polysaccharide that can be found in some marine algae (1). The polymer is linear and made up of repeating units of alternating β-D-galactopyranosil and 3,6-anhydro-α-l-galactopyranosil groups (2). Research has shown that agarose can generate excellent physical and biochemical conditions due to its biocompatibility (3). Agarose can also self-gel (generally based on temperature) through hydrogen bonding which makes it a popular polymer for gel synthetization (1). However, agarose gels are often very rigid and tough, making them popular for tissue engineering. They are also (much like all polysaccharide polymer hydrogels) often hydrophilic, making it difficult to achieve the controlled release of hydrophobic medicines. This research explains and analyzes hydrophobically modified agarose (HMA), as well as a novel fabrication process for HMA cryogels as well as initial testing to show the controlled release of hydrophobic medicines (4).

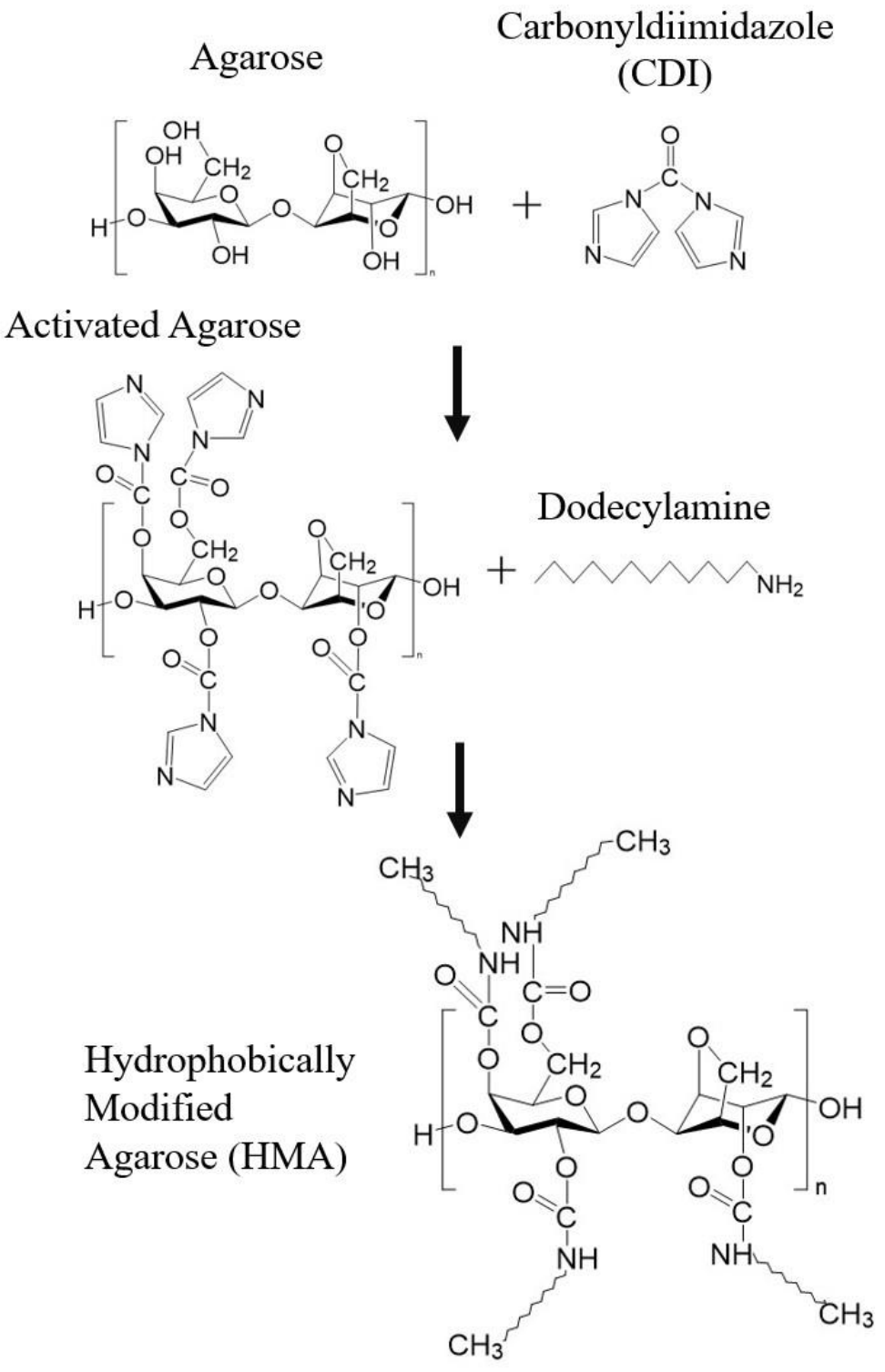

Figure 17: Chemical structure of activated agarose hydrophobically modified using Dodecylamine (4).

To hydrophobically modify agarose we first activated the hydroxyl groups in agarose (Figure 17). Once activated the hydroxyl groups could be bonded to a fatty amine. This process allowed the controlled development of hydrophobic micelles in water by varying the amount of fatty amine used and, as such, controlling the number of crosslinking points formed through hydrophobic interaction (known as the substitution degree). Moreover, a new method to prepare cryogels with a preset shape using HMA with very low solubility in water was also created.

Transdermal drug delivery (TDD) systems (which deliver therapeutic medicine through the skin) are one such use of micelle structures such as those formed in HMA cryogels. Using the micellular domains, HMA cryogels can encapsulate and protect therapeutic drugs. TDD systems that use synthetic micellular domains to adsorb and release hydrophobic medicine are common in relevant research. Polymer micelles formed from poly(ethylene glycol)–poly(amino acid) block copolymers were used to successfully adsorb indomethacin and resveratrol (which are hydrophobic drugs) and were also able to increase the amount of drug permeating the skin (5). Polymer micelles have also been formed from thiolated pluronic F127 and were used as a TDD system that could adsorb and release berberine hydrochloride (6). Block copolymer micelles we formed from poly(caprolactone)-block-poly(ethylene glycol) copolymer (PCL-b-PEG) and were able to adsorb and release retinal in vitro to porcine skin (7). Research has shown that synthetic polymers are the most widely used polymer for micelles creation (8). Because of this, we would like to contribute to micelle research by exploring micellular domains created from natural polymers.

3-2 MATERIALS AND METHODS

Materials

Low melting temperature agarose (melting temp. ≤ 65 °C, gelling temp. 26 °C – 30 °C) was purchased from Lonza (Rockland, ME, USA). Carbonyldiimidazole (CDI) and dodecylamine were purchased from Kanto Chemical Co. Inc. (Tokyo, Japan). Dimethyl sulfoxide (DMSO) was purchased from Wako Pure Chemical Industries Ltd. (Osaka, Japan). Mouse fibroblast L929 (RCB1451) cells were purchased from Riken Cell Bank (Tsukuba, Japan). The cells were maintained in a minimum essential medium containing 10% fetal bovine serum, 100 U/mL of penicillin, and 100 μg/mL of streptomycin, all purchased from Wako Pure Chemical Industries Ltd. (Osaka, Japan).

Synthesis of HMA

Through heating, agarose is dissolved in DMSO at a concentration of 5% (w/w) before being cooled to room temperature once fully dissolved. 1-carbonyldiimidazole is added and the solution is stirred at room temperature for 1 hour. To prevent precipitation, dodecylamine is dissolved first in DMSO before being added to the agarose solution. The agarose solution is then stirred at 25 °C for 12 hours. A dialysis membrane is used to dialyze the HMA solution against distilled water until the electrical conductivity of the HMA solution is the same as the distilled water. During this process, precipitation occurs as the DMSO in the agarose solution is replaced with distilled water. The gel precipitates are then removed from the membrane and immersed in 0.1 M sodium hydrogen carbonate buffer solution for

2 days at pH 8.5 and 37 °C. To neutralize 1-carbonyldiimidazole, a sodium hydrogen carbonate buffer solution was used. The buffer solution was regularly replaced. The precipitates were then immersed in distilled water and 99% ethanol for 1 day each at room temperature. The distilled water and the 99% ethanol were used to wash away the buffer solution and any unreacted solvents. The precipitates are then collected, pre-frozen in liquid nitrogen for 10 minutes, and then vacuum dried in a desiccator until no weight loss was observed. From previous research, the feeding ratio of dodecylamine to agarose was varied to obtain variances in the hydrophobicity (9,10). These variances can be observed in Table 2.

Table 2: Solubility, substitution degree, and contact angle of modified and unmodified agarose (4).

Sample	Solubility [a]		Feeding molar ratio of fatty amine to hydroxyl groups in agarose (%)	Substitution Degree (%)	Water contact Angle (Degrees)
	Water	DMSO			
Unmodified Agarose	+	+	-	-	71 ± 17
HMA2.5	+	+	2.5	0.1	82 ± 2
HMA5	+	+	5	0.8	104 ± 4
HMA10	-	+	10	3.0	106 ± 4
HMA100	-	-	100	-	-

[a] + and – indicate that the sample was soluble and insoluble, respectively.

To confirm the successful modification of HMA Fourier transform infrared spectroscopy (FT-IR, in ATR Mode, Spectrum One, Perkin Elmer, Waltham, MA, USA). The substitution degree was confirmed through hydrogen nuclear magnetic resonance (^{1}H-

NMR, JNM-GSX-400, JEOL Ltd., Tokyo, Japan). Modified and unmodified agarose as well as dodecylamine and CDI (1% w/v) was added to 1mL of DMSO-d6 and dissolved through heating. Data collected through the ^{1}H-NMR was inputted into the following formula to calculate the substitution degree:

$$Substitution\ Degree\ (\%) = \frac{\frac{\left(I_{H2-HMA} - \frac{I_{H2-Agr}}{I_{H1-Agr}}\right) \times I_{H1-HMA}}{72}}{I_{H1-HMA}} \times 100$$

Where $I_{H1\text{-}Agr}$ and $I_{H2\text{-}Agr}$ are the integral values of the H1 and H2 peaks of the unmodified agarose, and $I_{H1\text{-}HMA}$ and $I_{H2\text{-}HMA}$ are the H1 and H2 peaks of the HMA (Figure 18). The denominator, 72 was calculated based on the number of H2 molecules per alkyl group (18 molecules) in the modified portion of agarose multiplied by 4 which is the number of hydroxyl groups expected to be modified per unit of agarose.

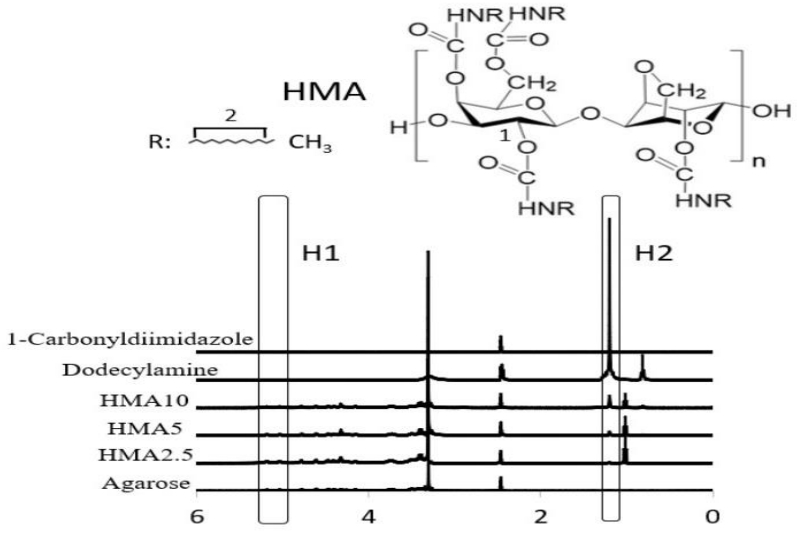

Figure 18: ^{1}H-NMR test of HMA (4)

Cryogel Synthesis

There were two methods used to synthesize cryogels made from modified and unmodified agarose. In Method 1, HMA and unmodified agarose were dissolved at 2% (w/v) in distilled water by stirring at 500 rpm and heating to 100 °C. The solution (1 mL) was dispensed into a 24-well plate and immersed in ice water (4°C) for 6 h once dissolved. The gel was removed from the well plate after 6 h (Figure 19).

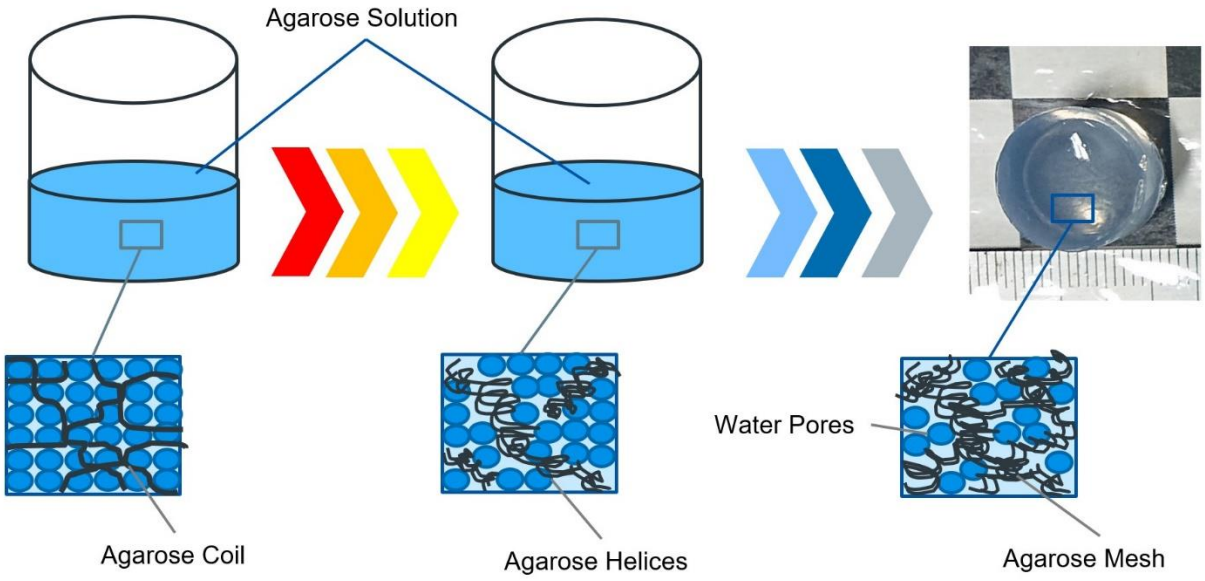

Figure 19: Fabrication of unmodified agarose cryogel using Method 1.

In Method 2 (cryogelation), HMA and unmodified agarose were dissolved at 2% (w/v) in DMSO (that has a freezing point of 18 °C) by stirring at 500 rpm and heating to 100°C. The solution (1 mL) was dispensed into a 24-well plate and immersed in icy water (4°C) to obtain solidification of the DMSO. Distilled water (2 mL cooled to 4°C) was added onto the solid polymer/DMSO construct and left for 30 min. The solid DMSO gradually dissolved

into the cold water during this period. The dissolved DMSO solution was then discarded, and 2mL of fresh cold distilled water was added and left again for 30 min. This process was repeated 10 more times to completely replace the DMSO with distilled water. Another 2 ml of fresh cold distilled water was added, and the mixture was stood at 4 °C for 6 h. The gel was removed from the well plate after 24 h (Figure 20).

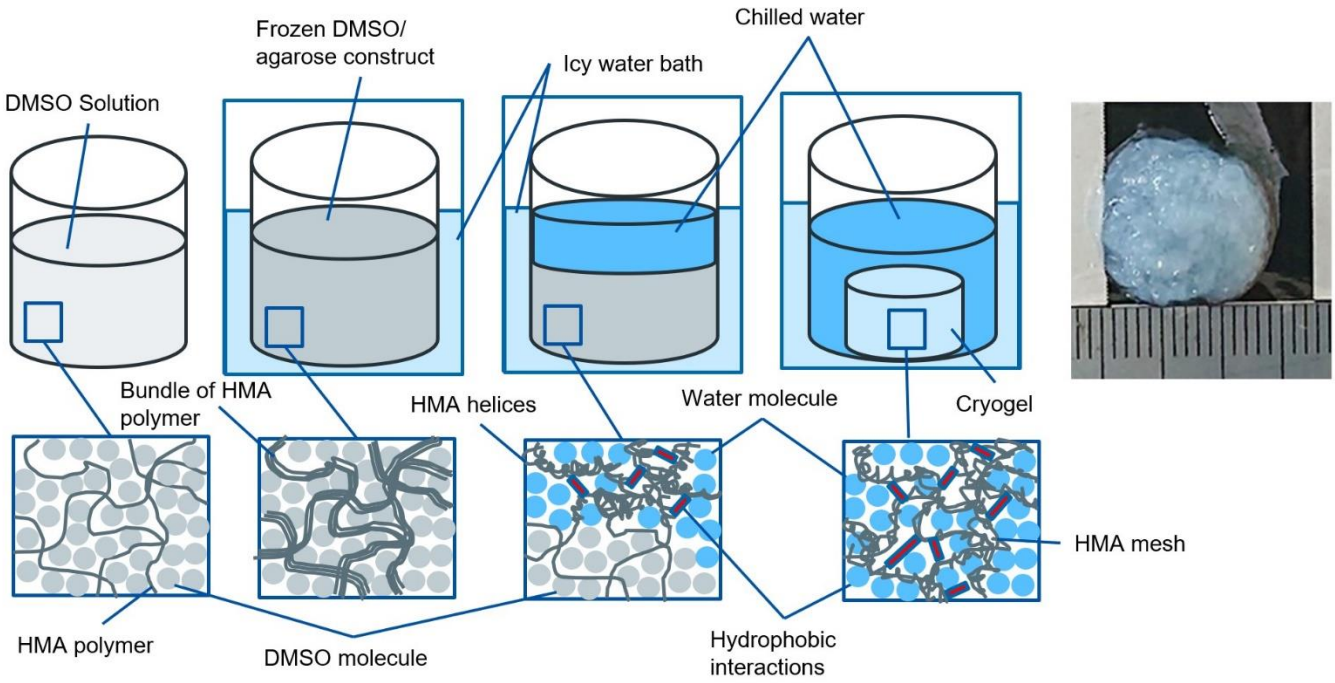

Figure 20: Fabrication of unmodified and modified agarose cryogels using Method 2.

Contact angle

A contact angle test was used to identify the hydrophobicity of unmodified and modified agarose. Through heating, we dissolved unmodified agarose and HMA in DMSO. The solutions were then evenly applied to glass slides and vacuum dried (within covered Petri dishes to prevent contamination) for 24 h. Droplets (1 µL) of ultrapure water were

dropped onto the glass slides. The angle between the droplet and the slide was then measured (DMe-200 Kyowa Interface Science Co. Ltd., Tokyo, Japan).

Mechanical properties

To identify the compressive Young's Modulus, a compression test was performed. Each sample was compressed at a rate of 5 mm/min on a Tensilon Universal Testing Machine using a 10N load cell (RTC-1210A, Oriented Co., Ltd., Tokyo, Japan). Young's Modulus was calculated from the first linear section of the stress-strain curve at a strain between 0% - 10%.

Cell adhesion and cytotoxicity

Cellular adhesion and cytotoxicity were first determined by using L929 fibroblast cells (11,12). In the first test, half of each 6-well cell culture plate was covered in a thin layer of unmodified and modified agarose cryogel. Cell suspension (1.0 mL, 4.0 x 10^4 cells/mL) was added to each well, and cells were observed under a microscope at 15 h and 48 h after cell seeding occurred.

To compare unmodified agarose hydrogels made using Method 1 to HMA10 cryogels a second adhesion and cytotoxicity test was performed. Cell suspension (2.91 × 105 cells/well) was added to a 6-well cell culture plate (3 mL per well). Of the 6-well culture plate, 3 wells were fully covered with a thin layer of unmodified agarose hydrogels and the other 3 were fully covered with a thin layer of HMA10 cryogels. After 4 h the cells that did not adhere to hydrogels/cryogels were counted. Then, the viability of the cells was examined by performing a trypan blue exclusion test.

Adsorption and release

The adsorption of eosin Y dye (Mw: 691.85 g/mol, octanol-water partition coefficient (log Pow) = 0. 18) was used to simulate hydrophobic medication, was observed. Eosin Y was dissolved in Ca2+- and Mg2+-free phosphate-buffered saline (PBS (-)) at a 1.0×10^{-6} mol/ml concentration. With a dry weight of 0.2g, HMA10 and agarose cryogels were prepared and added to the Eosin Y solution (5 mL). The cryogel solution was then shaken at 37 ° C and 100 rpm for a 24 h period during which samples of each solution (100 µL) were removed at certain intervals and the absorbance was measured using a UV/VIS spectrometer (wavelength of 517nm).

To determine the release behavior of the cryogels, after absorbance equilibrium was reached, the cryogels were placed into 4 mL of fresh PBS (-) and shaken at 37 °C and 80 rpm to release the adsorbed eosin Y. Over a 24 h period samples of the PBS (-) (50 µL) were taken and the absorbance was measured using a UV/VIS spectrometer. Every 6 h the PBS (-) was replaced. Based on the absorbance the cumulative release behavior of eosin Y (%) was identified.

Statistical Analysis

Data is presented as a mean ± standard deviation. Statistical differences among groups larger than three were analyzed using the one-way analysis of variance (ANOVA) with Bonferroni analysis.

3-3 RESULTS AND DISCUSSION

Previously, we hydrophobically modified gelatin and chitosan through the reductive amination of the aldehyde groups in fatty aldehydes and the amino groups found in both gelatin and chitosan (9,10). However, agarose doesn't have enough support to bond to. So, based on research conducted by Sakai et. al. (2007), to synthesize hydrophobically modified agarose, we first activated the hydroxyl groups of agarose using CDI and then formed covalent bonds between the hydroxyl groups and amino groups of the alkylamine (12).

FT-IR analysis (Figure 21) showed that the wavelength bands that denote the alkyl groups could be observed at 2927 cm-1 and 2855 cm-1. This band increases with the increase in substitution degree which indicates the successful modification of the hydroxyl groups in activated agarose with the alkyl chain.

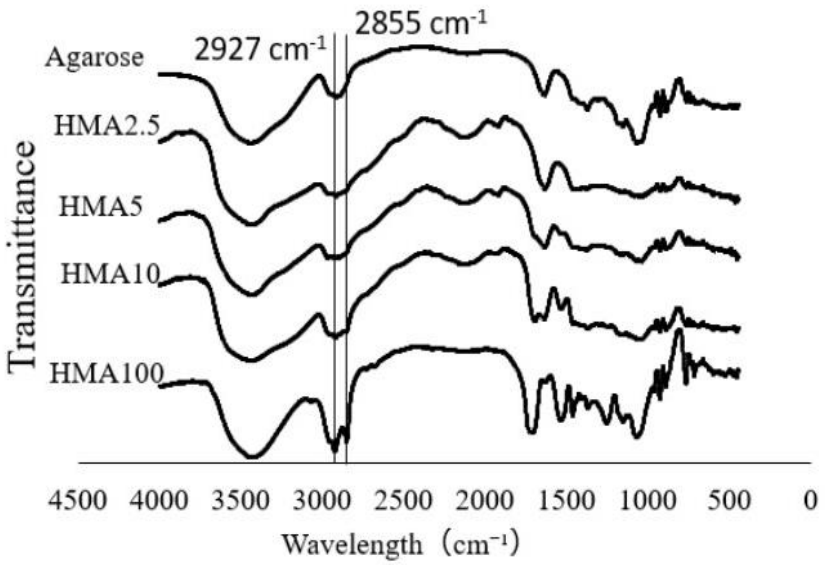

Figure 21: FT-IR results for HMA (4).

Table 2 shows the solubility of modified and unmodified agarose. It shows that while unmodified agarose, HMA2.5, and HMA5 could be dissolved in water, HMA10 and HMA100 could not. It is believed that the ability of unmodified and modified agarose to dissolve in water depends on the hydrophobic/hydrophilic nature of the sample – the stronger the hydrophobic nature of the sample the less likely it was to dissolve in water. Therefore, DMSO (which is amphiphilic) was used to dissolve modified and unmodified agarose, with all but the HMA100 successfully dissolving. Amphiphilic substances can interrupt hydrophobic interactions, allowing hydrophobic samples to dissolve. The reason HMA100 did not dissolve is likely because the HMA100 sample was too hydrophobic. It was discovered that any HMA with a substitution degree larger than 10% would not dissolve in DMSO. As such, a substitution degree and contact angle could not be empirically found for

HMA100. Due to this, all-further tests (except for the FT-IR and 1H-NMR tests) were completed on unmodified agarose and HMA10.

The substitution degree was determined by ^{1}H-NMR analysis (Table 2 and Figure 18). It was observed that as the feeding ratio of fatty amine to hydroxyl groups in agarose increased so too did the substitution degree.

The contact angle test showed that as the substitution degree in HMA samples increased so too did the contact angle. This agrees with what was seen in the ^{1}H-NMR analysis in Table 2.

Cryogel Preparation

Normally, agarose cryogels can be fabricated by dissolving the polymer in hot water and subsequently cooling down the aqueous agarose solution (Method 1) (1). Agarose is a polymer with molecules made up of strands that when heated separate into small coils. As the temperature lowers, these coils bond into pairs of helices. Once the temperature is below the melting point of agarose, these helices join into a mesh with pockets of water in between. Once the water is expelled, this mesh forms the skeleton of the cryogel while the pockets form into pores. As HMA10 is insoluble in water but does dissolve in DMSO, a new method to prepare cryogels by dissolving HMA in DMSO (Method 2) was derived. First, through heating, HMA10 was dissolved in DMSO. By lowering the temperature below the melting point of DMSO, the solution solidifies into an HMA/DMSO construct. Chilled distilled water (4°C) is added onto the construct which is being incubated in more cold water. Due to its low solubility in water, the addition of cold water does not affect the HMA10 but will affect the

solid DMSO causing it to dissolute into the water. If the DMSO melts during this process, cryogels with a predetermined shape could not be obtained. The cold water is exchanged with fresh cold water several times to completely dissolute the DMSO. This is because agarose is unable to self-gel when dissolved in concentrates of DMSO (14). DMSO prevents the balance needed between the crystalline interactions of polysaccharides and their amorphous solvents (14) and therefore needs to be replaced. Once the DMSO is replaced the environment becomes fully hydrophilic again which allows for the helices of agarose to form. During this phase, hydrophobic interactions will be also strongly exerted due to the hydrophilic environment (9).

Compression Testing

Although there was no statistical difference between the compressive strength of the unmodified or modified agarose cryogels made using method 1 and method 2, the average Young's Modulus of HMA10 cryogels (Method 2) is higher than that of unmodified agarose cryogels (Method 2) (Figure 22).

The higher overall compressive strength of HMA10 cryogels could be due to hydrophobic interaction between the hydrophobic alkyl groups. However, the use of DMSO as a solvent has likely weakened the hydrogen bonds that occur when agarose self-gels in water. Future research into using a different solvent or perhaps a mix of DMSO and something else could be experimented with to try and increase the mechanical properties.

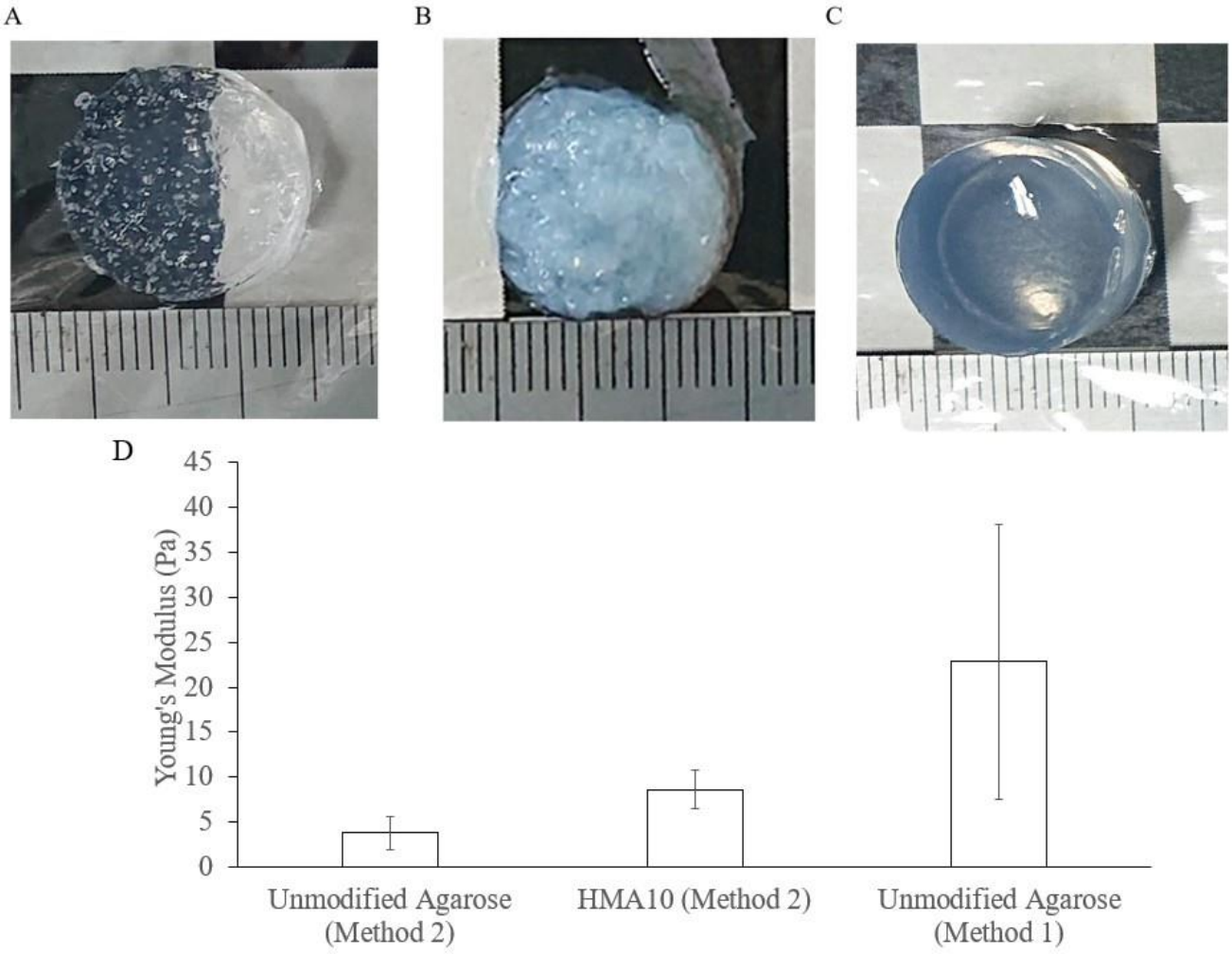

Figure 22: Unmodified agarose hydrogel prepared using Method 2 (A) HMA10 hydrogel prepared using Method 2 (B) and unmodified agarose hydrogel prepared using Method 1 (C). (D) Compression test of unmodified and modified agarose prepared using both Method 1 and Method 2 [n = 3] (4).

Cell Adhesion and Cytotoxicity

The first test was done to examine the cell adhesiveness of the HMA10 cryogel, L929 cells were seeded in a cell culture well plate partially covered with cryogel. Only a small number of cells had adhered to the cryogel after 48 h of cell seeding, showing low cellular

adhesiveness (Figure 23). Low cytotoxicity is assumed as the cells that adhered to the non-covered area proliferated.

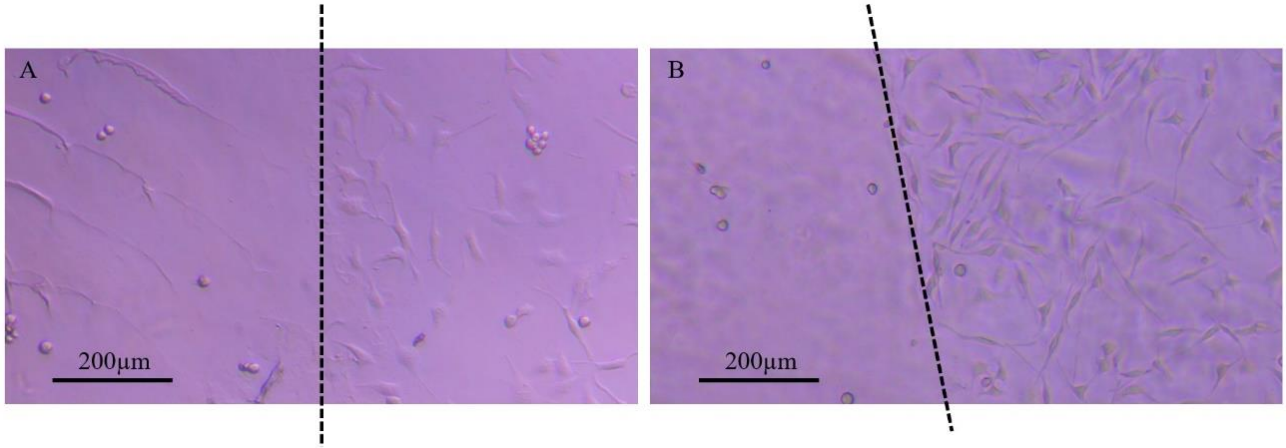

Figure 23: Cell adhesion of HMA10 at 24 hours (A) and 48 hours (B). The left side of the plate is covered with HMA10, and the right side of the plate is uncovered. [n = 3] (4).

Figures 24A and B show the results of the second test. Cell adhesion is shown in Figure 24A and shows that the adhesion of cells to HMA10 cryogels is low but that the average is greater than the cells adhered to the unmodified agarose cryogel. Agarose is bio-inert and does not have any sites for cells to adhere to which is likely why cell adhesion is so low (15). The likely reason that more cells adhered to the HMA10 cryogel is because of its hydrophobic nature (16,17). An important factor in cell adhesion is wettability (how hydrophobic or hydrophilic a surface is) (18). Ideal conditions for cell adhesion and proliferation occur on a moderately hydrophobic surface (contact angle of between 60° - 80°) (19). The hydrophobicity of HMA10 is likely a little too high for optimal cell adhesion and proliferation as it has a contact angle of 106°.

Figure 24B shows the number of viable cells. Between the HMA10 cryogel (Method 2) and unmodified agarose cryogels (Method 1), there is a negligible difference and quantitatively demonstrates that cytotoxicity is low.

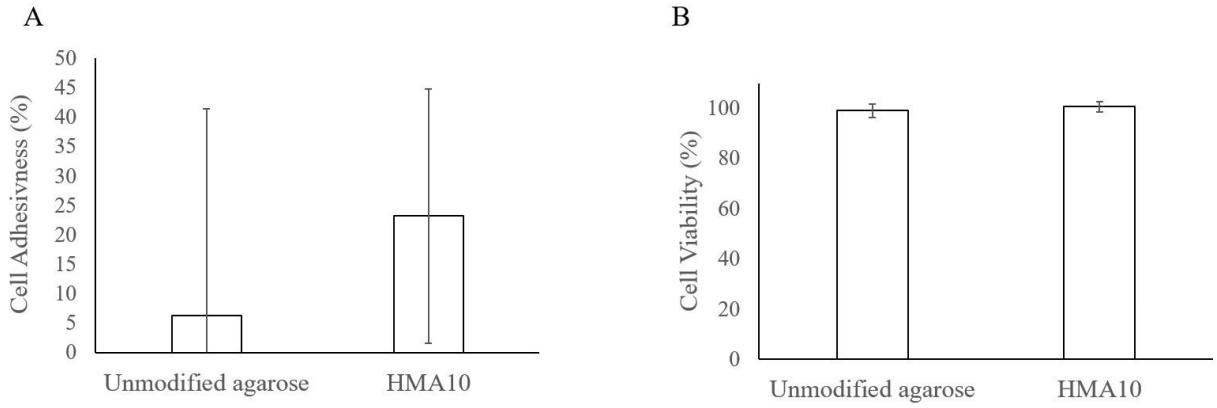

Figure 24: The percentage of cell viability in cell suspension from wells containing unmodified agarose, HMA10 and control liquid (A) and the percentage of cells adhered to unmodified agarose hydrogels (Method 1) and HMA10 hydrogels (Method 2) (B) [n = 3] (4).

Adsorption and diffusion

The adsorption (Figure 25A) showed that the amount of eosin-Y (a relatively hydrophobic dye) adsorbed to the HMA10 cryogel was much higher compared to the unmodified agarose cryogel.

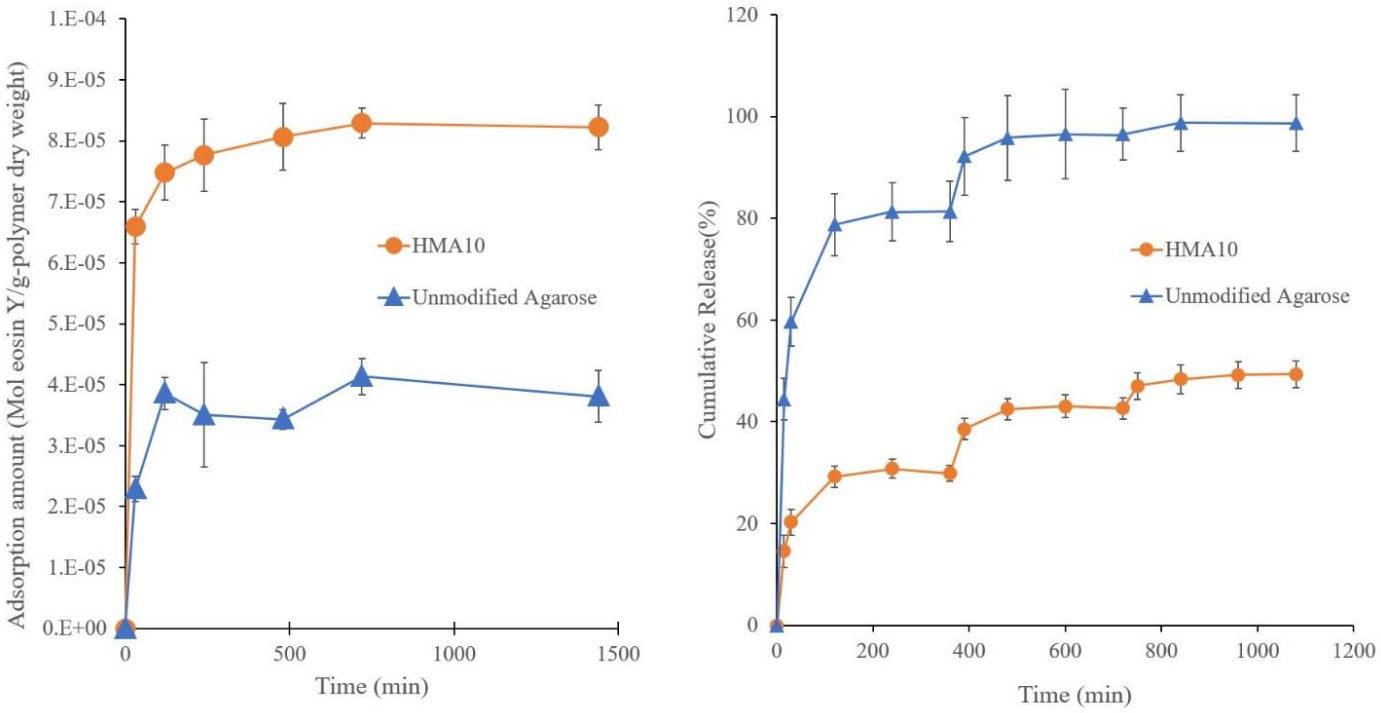

Figure 25: Adsorption (A) and release (B) of eosin-Y in HMA10 and unmodified agarose hydrogels [n = 3]. The PBS(-) was replaced at 360 and 720 min.

The release (Figure 25B) of eosin-Y into PBS showed that the HMA10 cryogel was released at a much more controlled rate than that of the unmodified agarose sample. Both tests suggested that the HMA10 cryogel can be used as a hydrophobic drug carrier.

We believe that a transdermal drug delivery (TDD) system would be the best use of the HMA cryogel because of the results of the compression test and the results of the adsorption and diffusion of eosin Y. Drugs can be passively diffused through the skin following either the intercellular or the transcellular route to be successfully adsorbed by the body (20). To be able to pass through the skin, drugs should be non-ionic, have low molecular weight, and be either hydrophilic (in certain conditions) or lipophilic (21). Lipophilic drugs

are drugs that dissolve in lipids (or oils) and are often hydrophobic (20). Lipophilic drugs can diffuse through the intercellular lipids in the skin (20). Hydrophobic drugs that have low molecular weight and are already available for use in TDD systems (such as fentanyl, clonidine, nitroglycerine, estradiol, etc.) should be able to be adsorbed into HMA cryogels.

In conclusion, by bonding the hydroxyl groups on agarose to the alkyl chains in fatty amines we were able to successfully increase the hydrophobicity of agarose. A new method to prepare cryogels from hydrophobic agarose (Method 2) was devised. However, samples with high hydrophobicity were insoluble and as such only, the HMA10 cryogel was examined. We found that the HMA10 cryogel had better controllability over the adsorption and diffusion of a hydrophobic dye than the unmodified agarose cryogel. These results show that HMA10 has the potential to be used as a biomaterial, specifically as a transdermal drug delivery system.

3-4 REFERENCES

1. **Spiller, K. L., Maher, S. A., Lowman, A. M.**: Hydrogels for the repair of articular cartilage defects, Tissue Eng. - Part B Rev., **17**, 281–299 (2011).

2. **Millán, A. J., Nieto, M. I., Moreno, R., Baudín, C.**: Thermogelling polysaccharides for aqueous gel casting - Part I: A comparative study of gelling additives, J. Eur. Ceram. Soc., **22**, 2209–2215 (2002).

3. **Zamora-Mora, V., Velasco, D., Hernández, R., Mijangos, C., Kumacheva, E.**: Chitosan/agarose hydrogels: Cooperative properties and microfluidic preparation, Carbohydr. Polym., **111**, 348–355 (2014).

4. **Evans, C., Morimitsu, Y., Nishi, R., Yoshida, M., Takei, T.**: Novel hydrophobically modified agarose cryogels fabricated using dimethyl sulfoxide, J. Biosci. Bioeng., **In Press**, https://doi.org/10.1016/j.jbiosc.2021.12.009 (2022).

5. **Yotsumoto, K., Ishii, K., Kokubo, M., Yasuoka, S.**: Improvement of the skin penetration of hydrophobic drugs by polymeric micelles, Int. J. Pharm., **553**, 132–140 (2018).

6. **Niu, J., Yuan, M., Chen, C., Wang, L., Tang, Z., Fan, Y., Liu, X., Ma, Y. J., Gan, Y.**: Berberine-loaded thiolated pluronic F127 polymeric micelles for improving skin permeation and retention, Int. J. Nanomedicine, **15**, 9987–10005 (2020).

7. **Laredj-Bourezg, F., Bolzinger, M. A., Pelletier, J., Valour, J. P., Rovère, M. R., Smatti, B., Chevalier, Y.**: Skin delivery by block copolymer nanoparticles (block copolymer micelles), Int. J. Pharm., **496**, 1034–1046 (2015).

8. **Zhang, H., Zhang, F., Wu, J.**: Physically crosslinked hydrogels from polysaccharides prepared by freeze–thaw technique, React. Funct. Polym., **73**, 923–928 (2013).

9. **Takei, T., Yoshihara, R., Danjo, S., Fukuhara, Y., Evans, C., Tomimatsu, R., Ohzuno, Y., Yoshida, M.**: Hydrophobically-modified gelatin hydrogel as a carrier for charged hydrophilic drugs and hydrophobic drugs, Int. J. Biol. Macromol., **149**, 140–147 (2020).

10. **Evans, C., Morimitsu, Y., Hisadome, T., Inomoto, F., Yoshida, M., Takei, T.**: Optimized hydrophobically modified chitosan cryogels for strength and drug delivery

systems, J. Biosci. Bioeng., **132**, 81–87 (2021).

11. **Fredrick, R., Podder, A., Viswanathan, A., Bhuniya, S.**: Synthesis and characterization of polysaccharide hydrogel based on hydrophobic interactions, J. Appl. Polym. Sci., **136**, 47665 (2019).

12. **Takei, T., Nakahara, H., Tanaka, S., Nishimata, H., Yoshida, M., Kawakami, K.**: Effect of chitosan-gluconic acid conjugate/poly(vinyl alcohol) cryogels as wound dressing on partial-thickness wounds in diabetic rats, J. Mater. Sci. Mater. Med., **24**, 2479–2487 (2013).

13. **Sakai, S., Hashimoto, I., Kawakami, K.**: Synthesis of an agarose-gelatin conjugate for use as a tissue engineering scaffold, J. Biosci. Bioeng., **103**, 22–26 (2007).

14. **Watase, M., Nishinari, K.**: Thermal and Rheological Properties of Agarose-Dimethyl Sulfoxide-Water Gels, Polym. J., **20**, 1125–1133 (1988).

15. **Cambria, E., Brunner, S., Heusser, S., Fisch, P., Hitzl, W., Ferguson, S. J., Wuertz-Kozak, K.**: Cell-Laden Agarose-Collagen Composite Hydrogels for Mechanotransduction Studies, Front. Bioeng. Biotechnol., **8**, 1–14 (2020).

16. **Chen, J. W., Lim, K., Bandini, S. B., Harris, G. M., Spechler, J. A., Arnold, C. B., Fardel, R., Schwarzbauer, J. E., Schwartz, J.**: Controlling the surface chemistry of a hydrogel for spatially defined cell adhesion, ACS Appl. Mater. Interfaces, **11**, 15411–15416 (2019).

17. **Ferrari, M., Cirisano, F., Carmen Morán, M.**: Mammalian cell behavior on

hydrophobic substrates: Influence of surface properties, Colloids and Interfaces, **3** (2019).

18. **Cai, S., Wu, C., Yang, W., Liang, W., Yu, H., Liu, L.**: Recent advance in surface modification for regulating cell adhesion and behaviors, Nanotechnol. Rev., **9**, 971–989 (2020).

19. **Wei, J., Yoshinari, M., Takemoto, S., Hattori, M., Kawada, E., Liu, B., Oda, Y.**: Adhesion of mouse fibroblasts on hexamethyldisiloxane surfaces with a wide range of wettability, J. Biomed. Mater. Res. - Part B Appl. Biomater., **81**, 66–75 (2007).

20. **Shaker, D. S., Ishak, R. A. H., Ghoneim, A., Elhuoni, M. A.**: Nanoemulsion: A review on mechanisms for the transdermal delivery of hydrophobic and hydrophilic drugs, Sci. Pharm., **87**, 17 (2019).

21. **Prausnitz, M. R., Langer, R.**: Transdermal drug delivery, Nat. Biotechnol., **26**, 1261–1268 (2008).

Chapter 4 *Isotherms, Kinetics and Thermodynamics of HMC and HMA Cryogels*

4-1 INTRODUCTION

Research into the mechanisms of adsorption has been extensive across a range of disciplines. Mostly, research focuses on the removal of toxic dyes and heavy metals from wastewater however, a recent increase in the understanding of the adsorption process of biomaterials has also occurred. Understanding the adsorption process is vital when designing adsorbents.

Research surrounding adsorption mostly focuses on isotherms, kinetics, and thermodynamic processes (1). Isotherms, both practical (the equilibrium isotherm) and theoretical (Langmuir's and Freundlich's isotherms) isotherms focus on understanding the relationship between the amount of adsorbate adsorbed per amount of adsorbent and the concentration of the adsorbate at a specific temperature (2). Kinetics (for example the pseudo-first and second-order) focus on determining the time an adsorbent takes to adsorb an adsorbate (1). Finally, thermodynamic processes can provide an understanding of the spontaneity of the processes involved as well as any heat exchanges that might occur (3).

In previous research, we developed hydrophobically modified chitosan (HMC) cryogels (4) and hydrophobically modified agarose (HMA) cryogels (5) to be used as biomaterials. A further understanding of the adsorption processes undertaken by HMC and HMA cryogels is the focus of this research. Particularly we are interested in investigating the

equilibrium, Langmuir's and Freundlich's isotherms as well as the kinetic and thermodynamic processes that occur when both gels are adsorbing hydrophobic dyes.

4-2 MATERIALS AND METHODS

Materials

Chitosan (degree of deacetylation 81%; viscosity average molecular weight 1.5x105 Da, Chitosan LL) was kindly donated by Yaizu Suisankagaku Industries (Shizuoka, Japan). Dodecanal was obtained from Wako Pure Chemical Industries Ltd. (Osaka, Japan). 2-Picolineborade was purchased from Junsei Chemical Co. Ltd. (Tokyo, Japan). Rhodamine B (MW: 479.02, Color Index Number: 45,170, MF: $C_{28}H_{31}C_lN_2O_3$) (Figure 26A) was purchased from Tokyo Chemical Industry (Tokyo, Japan).

Low melting temperature agarose (melting temp. ≤ 65 °C, gelling temp. 26 °C – 30 °C) was purchased from Lonza (Rockland, ME USA). Carbonyldiimidazole (CDI) and dodecylamine were purchased from Kanto Chemical Co. Inc. (Tokyo, Japan). Dimethyl sulfoxide (DMSO) was purchased from Wako Pure Chemical Industries Ltd. (Osaka, Japan). Eosin Y (MW: 691.85, Color Index Number: 45,380, MF: $C_{20}H_6Br_4Na_2O_5$) (Figure 26B) was also purchased from Wako Pure Chemical Industries Ltd. (Osaka, Japan).

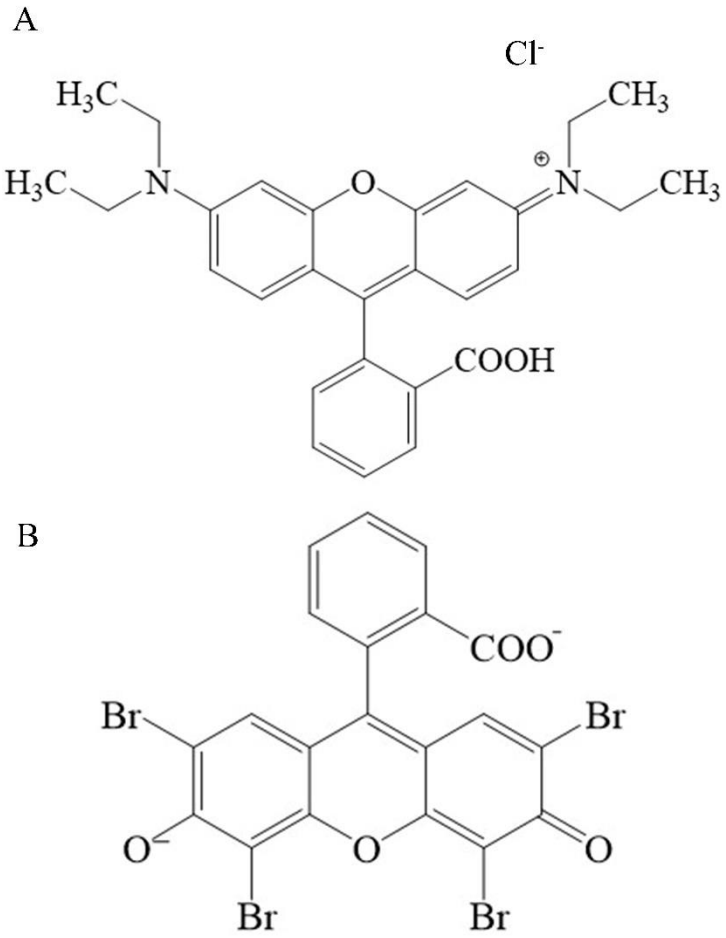

Figure 26: A) Chemical structure of rhodamine B and B) the chemical structure of eosin Y.

Fabrication of hydrophobically modified chitosan cryogels

Hydrophobically modified chitosan (HMC) was formed when fatty aldehydes were bonded to the amino groups in chitosan through imide bonding followed by reduction (4). HMC was dissolved in an aqueous hydrochloric acid (HCL) solution at 0.1 M (mol/L) to produce HMC (1 %) cryogels. The pH of the acidic solution was then increased to 7.0 by

adding sodium hydroxide (NaOH). Samples were frozen (-30 °C) in cylindrical molds for longer than 6 hours after which they were thawed for 2 hours.

Fabrication of hydrophobically modified agarose cryogels

Hydrophobically modified agarose (HMA) was created by first activating the carboxyl groups in agarose (using CDI). Then a covalent bond between the carboxyl groups and the amino groups in the fatty aldehyde was formed (5). HMA cryogels were fabricated by dissolving 2% (w/v) of HMA in DMSO. The HMA solution was distributed into a 24-well plate (1 mL per well) and immersed in icy water (4 °C). Added to each well was 1 mL of distilled water (cooled to 4 °C) and the mixture was left to stand for 30 min. The liquid in each well was then thrown out and fresh distilled water was added and again the solution was left for 30 min. This process was repeated 10 times before a further 2 mL of cooled distilled water was added, and the mixture was stood in icy water (4 °C) for 6 h allowing for HMA cryogels to form.

Adsorbate preparation of rhodamine B

A stock solution of rhodamine B was prepared by dissolving 0.048 g of dye into 10 mL of PBS to give a concentration of 52.69 g/L. The stock solution was further diluted with PBS to give the concentrations seen in Table 3.

Table 3: Adsorbate concentrations of rhodamine B for HMC experiments.

Sample	Concentration
Stock	52.69 g/L
Concentration 1	3.59 g/L
Concentration 2	1.8 g /L
Concentration 3	718.54 mg/L
Concentration 4	359.27 mg/L
Concentration 5	35.93 mg/L
Concentration 6	17.96 mg/L

Adsorbate preparation of eosin Y

A stock solution of Eosin Y was prepared by dissolving 0.363 g of dye into 10 mL of PBS to give a concentration of 24.22 g/L. The stock solution was further diluted with PBS to give the concentrations seen in Table 4.

Table 4: Adsorbate concentrations of eosin Y for HMA experiments.

Sample	Concentration
Stock	24.22 g/L
Concentration 1	698.86 mg/L
Concentration 2	345.9 mg/L
Concentration 3	138.37 mg/L
Concentration 4	34.5 mg/L
Concentration 5	6.92 mg/L

Adsorption experiment of HMC

The adsorption equilibrium was determined by placing one HMC cryogel into each glass vial which contained 200 µL of dye solution. Each cryogel contained 0.010 g of dried HMC polymer and 100 µL of distilled water. The vials were shaken at 100 rpm for 24 hours at a specific temperature (277.15 K, 293.15 K, and 310.15 K) to allow for equilibrium.

Samples were taken at various intervals and the concentration of Rhodamine B was determined using a microplate reader (Infinite 200 Pro Mplex) at 554 nm.

The adsorption kinetics was conducted by placing one HMC cryogel into each glass vial which contained 1 mL of dye solution. Each cryogel contained 0.010 g of dried HMC powder and retained 100 µL of distilled water. The vials were shaken for 24 h at 100rpm at a specific temperature (277.15 K, 293.15 K, and 310.15 K) to allow for equilibrium to be reached. Samples were taken at various intervals and the concentration of rhodamine B was determined using a microplate reader (Infinite 200 Pro Mplex) at 554 nm.

Adsorption experiment of HMA

Adsorption experiments were conducted at a constant speed of 100 rpm using 20 mL graduated glass vials with screw lids. Adsorption measurements were conducted at various time intervals and temperatures (277.15 K, 293.15 K, and 310.15 K).

The adsorption equilibrium was ascertained by placing one HMA cryogel into each glass vial which contained 500 µL of eosin Y dye solution. Each cryogel contained 0.020 g of dried HMA powder and retained 400 µL of distilled water. The vials were shaken for 24 hours at a specific temperature to allow for equilibrium between the eosin Y solution and the cryogel to be achieved. Samples were taken at various intervals and the concentration of eosin Y was determined using a Nanodrop-8000 reader (Thermo, SCIENTIFIC) at 517 nm

The adsorption kinetics was ascertained by placing one HMA cryogel into each glass vial which contained 200 µL of dye solution. Each cryogel contained 0.020 g of dried HMA powder and retained 500 µL of distilled water. The vials were shaken for 24 h at a specific

temperature to allow for equilibrium to be achieved. Samples were taken at various intervals and the concentration of eosin Y was determined using a Nanodrop-8000 reader (Thermo, SCIENTIFIC) at 517 nm.

4-3 RESULTS AND DISCUSSION

Adsorbate preparation

To identify the chemical processes that both HMC and HMA cryogels undergo during the adsorption of hydrophobic dyes, eosin Y and rhodamine B dyes (in different concentrations) were used. The decision to use different dyes (with different octanol-water partition coefficient values) at different concentrations was made due to the initial testing performed on HMC and HMA cryogels (4,5). This initial testing showed that while eosin Y was an acceptable dye for HMA cryogels, it was not acceptable for HMC cryogels because eosin Y has a negative charge and chitosan has a positive charge. The hydrophobic modification did not alter the charge and as such, hydrophobic adsorption could not be proven due to the possibility of ionic bonding taking place. On the other hand, rhodamine B is acceptable for use with HMC cryogels due to its neutral charge, however, initial testing showed that it was unsuitable for use with HMA cryogels due to its highly hydrophobic nature. As such, to obtain the most truthful data to clarify the chemical processes that both HMC and HMA experience, it was decided that individual dyes for each gel should be used and a comparison between the two types of cryogels would not be carried out.

Isotherm calculations

The amount of rhodamine B and eosin Y adsorbed at equilibrium q_e (mg/g of dried cryogel) was calculated using the following equation:

$$q_e = \frac{C_o - C_e}{m} \times V$$

where C_o is the initial concentration of dye solution (mg/L), C_e is the concentration of dye solution at equilibrium (mg/L), m is the mass of dried cryogel (g), and V is the initial volume of the aqueous die solution (L). Figure 27 shows the equilibrium isotherms for HMC and HMA cryogels at different concentrations of dye and different temperatures.

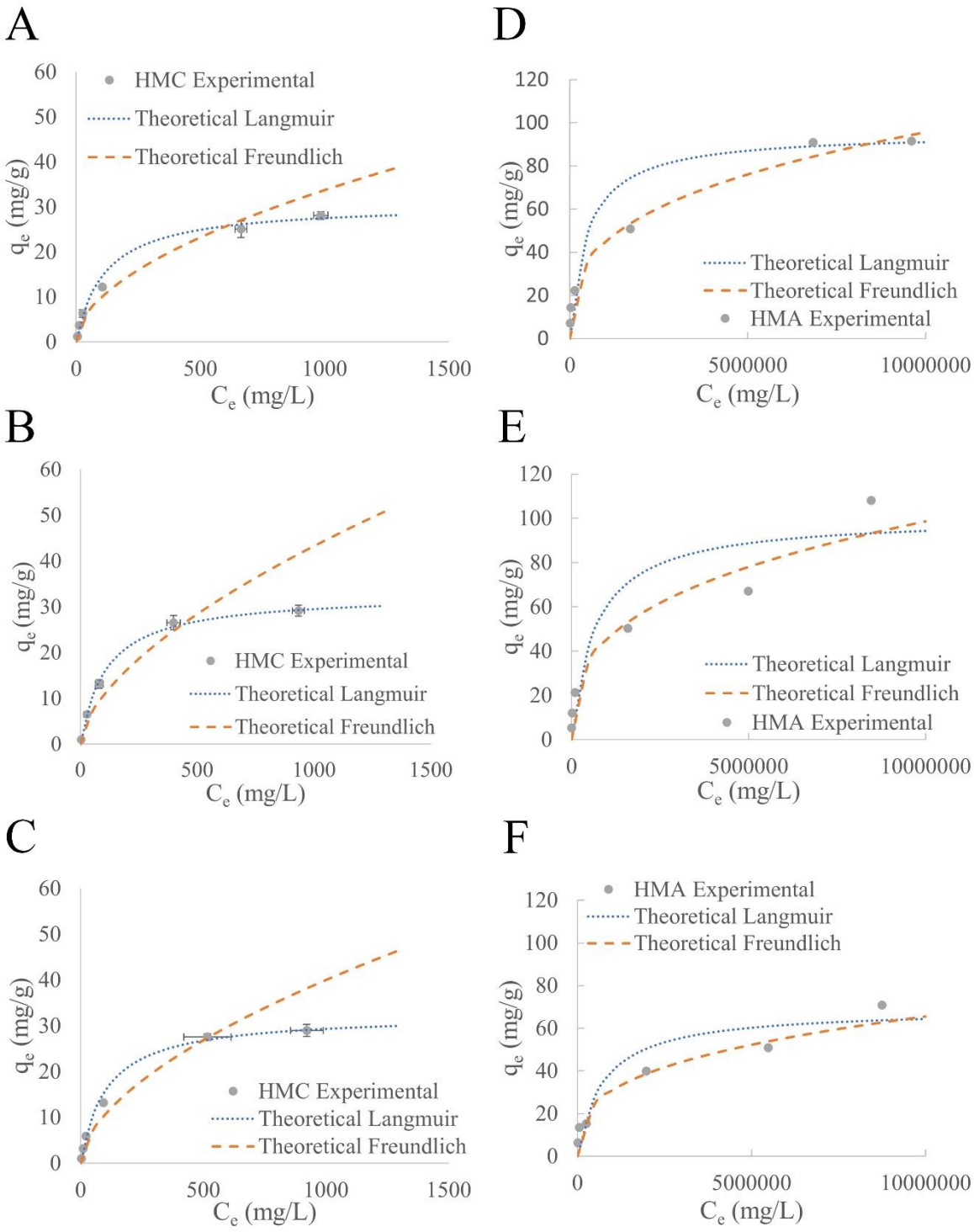

Figure 27: Extrapolated curves of Langmuir's and Freundlich's isotherms compared to the experimental equilibrium data for A) HMC at 277.15 K, B) HMC at 293.15 K, C) HMC at 310.15 K, D) HMA at 277.15 K, E) HMA at 293.15 K, and F) HMA at 310.15 K. [n = 3]

Langmuir's isotherm is a theoretical model used to describe the equilibrium between the adsorbate and the adsorbent systems (3,6,7). Langmuir's assumes that the surface of the adsorbent has a limited number of adhesion locations and that each location can only adhere to one molecule (3,6,7). It also assumes that the molecules do not interact with each other, which means that only a single or monolayer of molecules can attach to the surface of the adsorbent (3,6,7). The following equation is used to identify Langmuir's adsorption capacity q_l (mg of dye/g of dried cryogel):

$$q_l = \frac{q_{max} \times K_L \times C_e}{1 + K_L \times C_e}$$

where C_e is the equilibrium concentration (mg/L), K_L is Langmuir's constant (L/mg of dye), and q_{max} is the maximum Langmuir's adsorption capacity (mg of dye/g of dried cryogel). To determine q_{max} and K_L, C_e is plotted against C_e/q_e (where q_e is the amount of dye adsorbed at equilibrium (mg/g of dried cryogel)) (Figure 28).

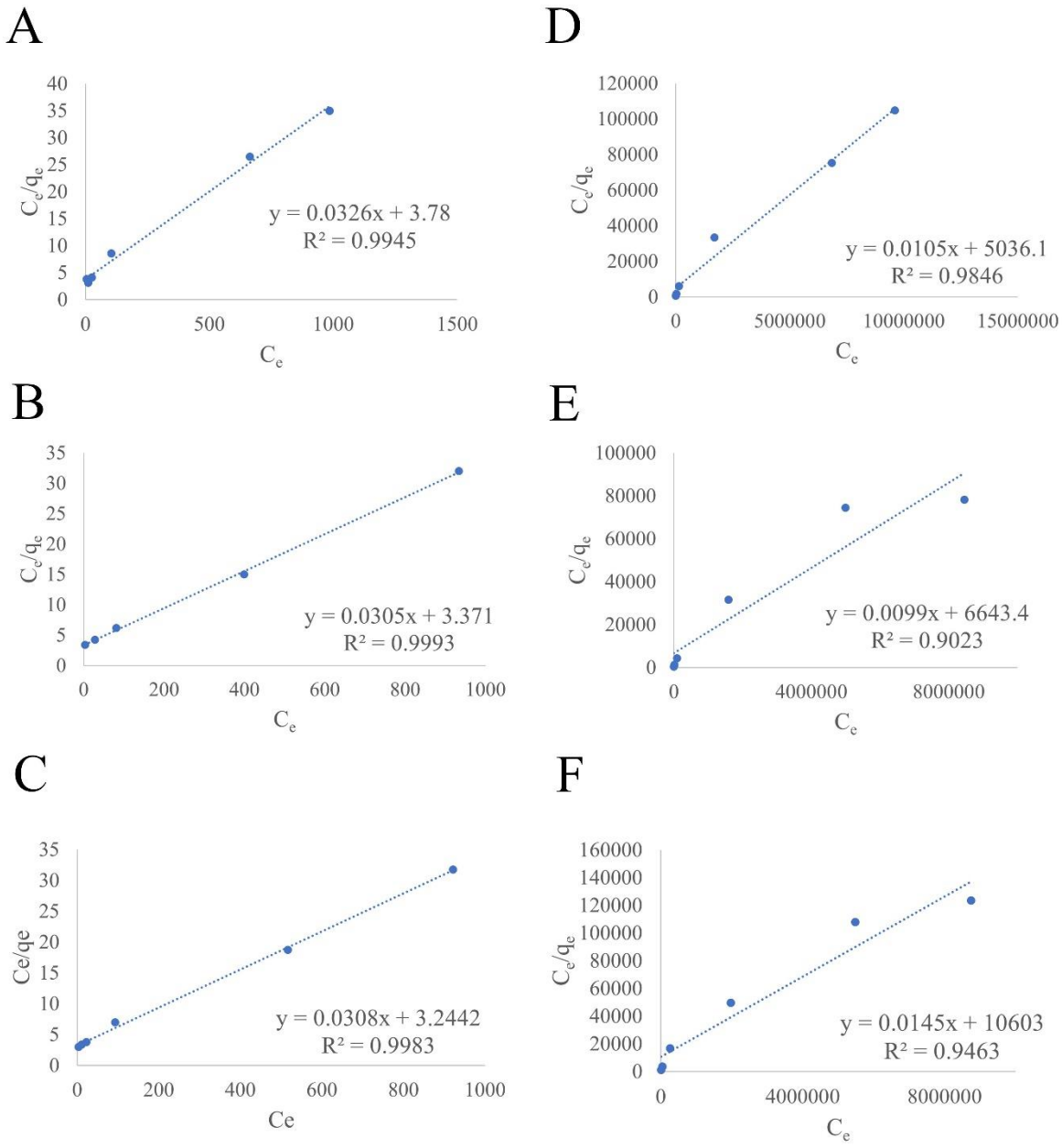

Figure 28: Plot of C_e/q_e vs. C_e to determine q_{max} and K_L of HMC and HMA cryogels. A) HMC at 277.15K, B) HMC at 293.15K, C) HMC at 310.15K, D) HMA at 277.15K, E) HMA at 293.15K and F) HMA at 310.15K.

Freundlich's isotherm is an empirical representation of the relationship between the concentration of the solute adsorbed on the absorbent and the concentration of the adsorbate

in the liquid phase (2,7,8). Freundlich assumes again that there is a limited amount of adherence locations on the surface of the adsorbate but that interaction between molecules is possible thereby allowing for multiple layers of molecules to be adsorbed (2,8). The following equation was used to identify Freundlich's adsorption capacity q_f (mg of dye/g of dried cryogel):

$$q_f = K_F \times C_e^{\frac{1}{n}}$$

where K_F is Freundlich's constant ((mg of dye/g of dried cryogel) (mg/L of dye solution)^n), C_e is the concentration at equilibrium (mg/L), and *1/n* is the heterogeneity of the cryogels surface. To determine K_F and *1/n*, Log q_e is plotted against Log C_e (where q_e is the amount of dye adsorbed at equilibrium (mg/g of dried cryogel)) (Figure 29).

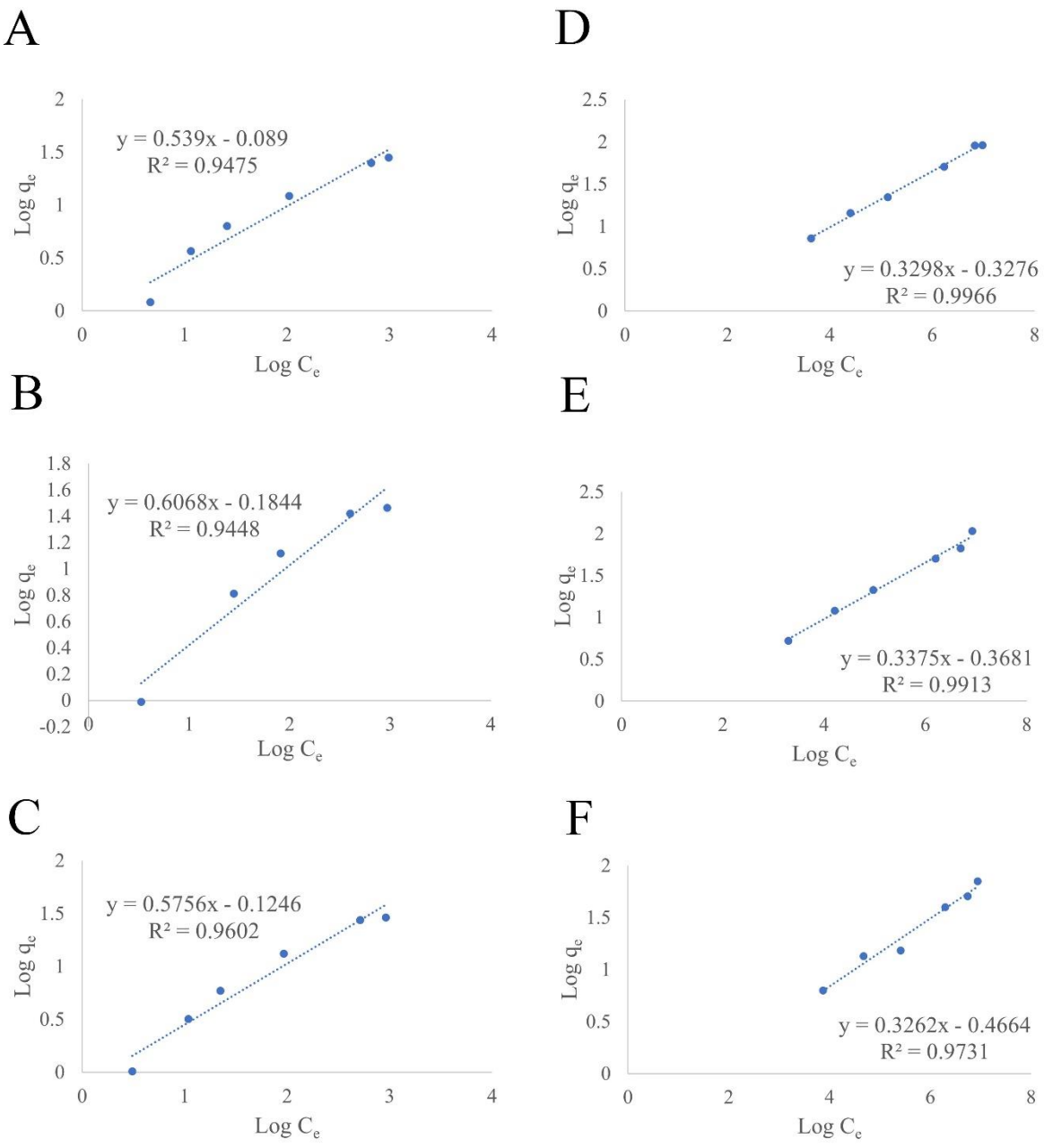

Figure 29: Plot of Log q_e vs Log C_e to determine K_F and 1/n of HMC and HMA cryogels. A) HMC at 277.15K, B) HMC at 293.15K, C) HMC at 310.15K, D) HMA at 277.15K, E) HMA at 293.15K and F) HMA at 310.15K.

Tables 5 and 6 and Figure 27 show the results of the equilibrium, Langmuir's, and Freundlich's isotherms for HMC and HMA. The experimental values obtained for HMC cryogels match very well with the curve extrapolated from Langmuir's theoretical model (shown in Figure 27) indicating that the relationship between the HMC cryogel and rhodamine B is likely to be monolayer and that it is likely no interaction between rhodamine B molecules (10). It also indicates that the surface of HMC cryogels is likely homogenous (10) and (as seen in Table 5 and Figure 27) as the temperature increases so too does the adsorbed amount of rhodamine B. The determination coefficient (R^2) shown in Table 5 also shows that the experimental data is a closer match to Langmuir's model at all temperatures, compared to Freundlich's model.

On the other hand, the experimental values obtained for HMA cryogels match closer to Freundlich's theoretical model (Table 6 and Figure 27) indicating the likelihood of multiple layers of eosin Y bonding to the HMA cryogels and/or interactions occurring between neighboring eosin Y molecules. It also indicates that the surface of HMA cryogels is likely heterogeneous (9). The determination coefficient (R^2) shown in Table 6 also shows that the experimental data is a closer match to Freundlich's model at all temperatures, compared to Langmuir's model.

From 1/n, adsorption conditions can be estimated and because 1/n is more than 0 but less than 1, adsorption is favorable for both HMA and HMC cryogels (Tables 5 and 6) (2).

Table 5: Langmuir's and Freundlich's parameters for HMC.

Isotherm models	Isotherm parameters	HMC		
		Temperature (K)		
		277.15	293.15	310.15
Langmuir	K_L (L/mg)	0.0086	0.0090	0.0095
	q_{max} (mg/g)	30.703	32.790	32.452
	R^2	0.9945	0.9993	0.9983
Freundlich	K_F (mg/g) $(mg/L)^n$	0.8146	0.6540	0.7506
	1/n	0.5389	0.6068	0.5756
	R^2	0.9475	0.9448	0.9602

Table 6: Langmuir's and Freundlich's parameters for HMA

Isotherm models	Isotherm parameters	HMA		
		Temperature (K)		
		277.15	293.15	310.15
Langmuir	K_L (L/mg)	2.082×10^{-6}	1.496×10^{-6}	1.365×10^{-6}
	q_{max} (mg/g)	95.3731	100.6366	69.1152
	R^2	0.9846	0.9023	0.9463
Freundlich	K_F (mg/g) $(mg/L)^n$	0.4703	0.4284	0.3416
	1/n	0.3298	0.34	0.3261
	R^2	0.9966	0.9913	0.9731

Thermodynamic calculations

While the isotherms above are used to identify how and in what way the hydrophobic dye is adsorbed to the gel, thermodynamics can be used to determine the interrelationships between the heat, work, and energy of a system at equilibrium. There are three laws of thermodynamics. We are interested in the first law which states that energy and matter can be neither created nor destroyed; only transformed from one form to another.

A part of the first and second laws of thermodynamics is Gibbs free energy which states that the combination of entropy (a measurement of randomness), temperature, and enthalpy (a measurement of heat) explains whether a reaction is going to be spontaneous or not (7,9,11). If a reaction is spontaneous, Gibbs's free energy is negative and indicates that the process does not need any extra energy to begin. If a reaction is not spontaneous, Gibbs's free energy is positive and indicates that something is needed to start the process (12). The change in Gibbs free energy when a system is at equilibrium is represented by this equation:

$$\Delta G^\circ = \Delta H^\circ - T \times \Delta S^\circ$$

where ΔG° is the change in Gibbs free energy (kJ/mol), ΔH° is the change in enthalpy (kJ/mol), T is the temperature (Kelvin) and ΔS° is the change in entropy (J/mol·K). The following equation is used to identify Gibbs Free Law:

$$\Delta G^\circ = -R \times T \times \ln K_D$$

where R is the gas constant (J/mol·K) and K_D is the equilibrium constant. Langmuir's constant (K_L) can be used to calculate K_D. However, K_D is unitless, so K_L (L/mg of dye) is converted to L/mol of dye by multiplying by the molar mass (g/Mol of dye) of rhodamine B or eosin Y and 1000. K_L is then multiplied by 55.5 mol/L which is the molecular weight of water to make it unitless (7,13). Table 7 shows the results of the calculated Gibbs free energy.

Table 7 shows that Gibbs's free energy is negative for both HMC and HMA cryogels indicating that the adsorption process is spontaneous. HMC cryogels have a positive change in enthalpy indicating that the processes in endothermic whereas in the HMA cryogels have a negative change in enthalpy indicating that the process is exothermic. The adsorption

process should be exothermic however there has been previous research into chitosan hydrogels (13) and rhodamine B (14) that has shown the process to be endothermic. So far, the reason for this has not been stated. It is also possible that as these conclusions are formed based on data obtained through theoretical calculations, they may not reflect what is occurring under experimental conditions.

Table 7: Thermodynamic constants for HMC and HMA

	Thermodynamics Constant	Temperature (K)		
		277.15 K	293.15 K	310.15 K
HMC	K_D	229070.63	237286.49	252518.26
	ΔG° (kJ/mol)	-28.44	-30.17	-32.08
	ΔH° (kJ/mol)		2.105	
	ΔS° (J/ (mol · K))		110.16	
HMA	K_D	79.94	57.43	52.40
	ΔG° (kJ/mol)	-10.095	-9.873	-10.208
	ΔH° (kJ/mol)		-9.192	
	ΔS° (J/ (mol · K))		2.95	

Kinetics calculations

Kinetics describes the rate at which a particular process occurs and the expected pathway by which the process will occur (1,16). The below linear equation is used to determine the pseudo first order adsorption capacity over time q_t (mg/g of cryogel):

$$\ln(q_e - q_t) = \ln q_e - k_1 \times \mathrm{t}$$

where q_e is the adsorption capacity at equilibrium (mg/g of cryogel), q_t is the adsorption capacity at the time, *t* (mg/g of cryogel), k_1 is the adsorption rate constant, and *t* is the time (min).

The linear equation for the pseudo second order adsorption capacity over time q_t (mg/g of cryogel) is shown below:

$$\frac{t}{q_t} = \frac{1}{k_2 \times {q_e}^2} + \frac{1}{q_e} \times t$$

where t is time (h), q_t is the adsorption capacity at the time, t (mg/g of cryogel), q_e is the adsorption capacity at equilibrium (mg/g of cryogel), and k_2 is the adsorption rate constant.

Table 8: Pseudo first and second order parameters for HMC and HMA.

			Pseudo First Order		Pseudo Second Order	
	Temperature	q_e (mg/g)	k_1 (1/h)	R^2	k_2 (mg/ (g · h))	R^2
HMC	277.15 K	16.2	15.67	0.92	0.48	0.9982
	310.15 K	25.1	9.50	0.94	1.70	0.9995
HMA	277.15 K	127.2	2.42	0.93	0.108	0.9997
	310.15 K	114.7	2.54	0.80	0.144	0.9995

Table 8 and Figure 30 show the pseudo first order and pseudo second order results for HMC and HMA cryogels. Both HMC and HMA gels at both temperatures showed a similar trend. Before equilibrium was reached (when time (t) is less than 1 hour) both HMC and HMA gels fit better with the theoretical curve extrapolated from the pseudo first order equation. However, after equilibrium is reached, both HMC and HMA gels fit better to the theoretical curve extrapolated from the pseudo second order equation. Figure 30 also shows that the adsorption equilibrium is reached quite quickly and that the adsorption capacity for

HMC cryogels is higher at higher temperatures and for HMA cryogels is higher at lower temperatures.

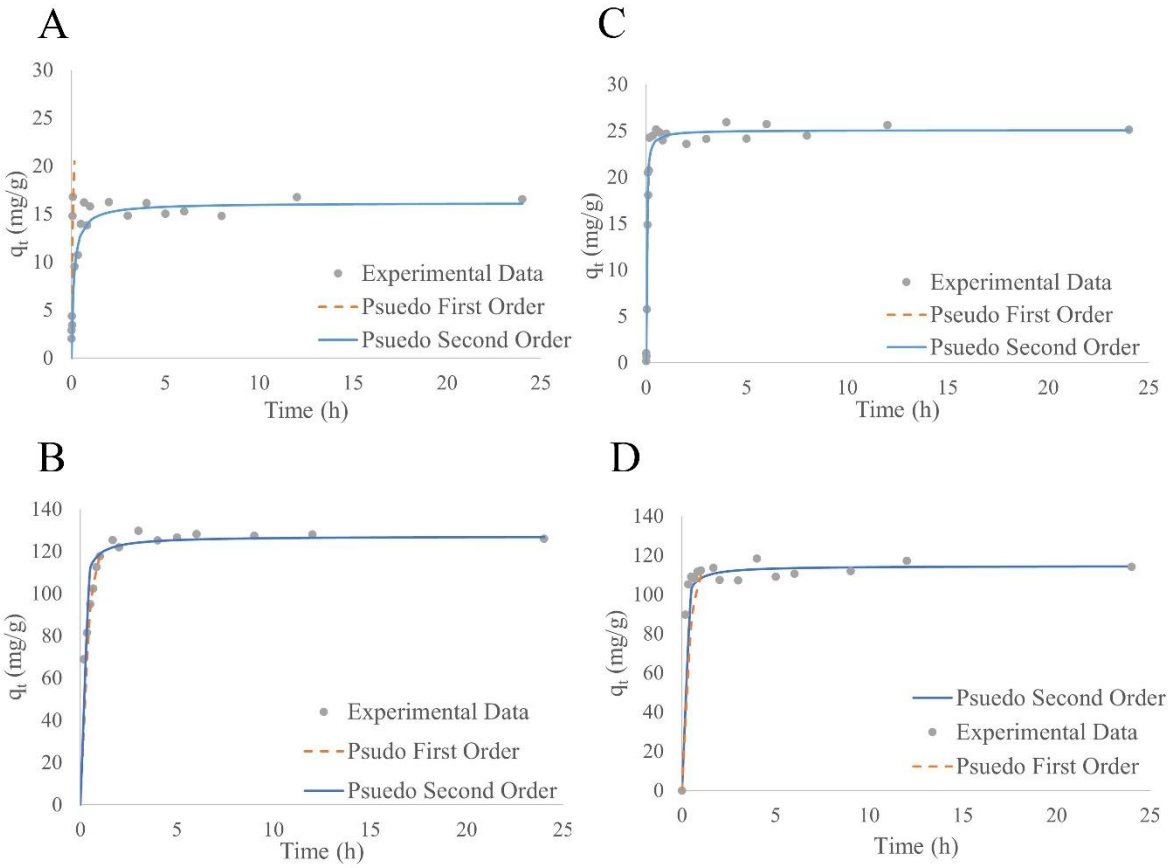

Figure 30: Comparison of the experimental, pseudo first and pseudo second orders for A) HMC at 277.15 K, B) HMA at 277.15 K, C) HMC at 310.15 K and D) HMA at 310.15 K. [n=3]

In conclusion, this research attempted to better understand the chemical processes that HMC and HMA cryogels undergo when adsorbing hydrophobic dyes. It was discovered that Langmuir's isotherm was better suited to HMC cryogels whereas Freundlich's isotherm better explained HMA cryogels. Both HMC and HMA cryogels had a negative change in Gibbs free energy indicating that the adsorption process begins spontaneously. Kinetics showed that adsorption happened very quickly, is temperature dependent, and that both HMC

and HMA cryogels fit best to the pseudo first order theoretical model before equilibrium is reached and that after equilibrium is reached the pseudo second order theoretical model is a better fit.

4-4 REFERENCES

1. **Lin, J., Wang, L.**: Comparison between linear and non-linear forms of pseudo-first-order and pseudo-second-order adsorption kinetic models for the removal of methylene blue by activated carbon, Front. Environ. Sci. Eng. China, **3**, 320–324 (2009).

2. **Zhou, C., Wu, Q., Lei, T., Negulescu, I. I.**: Adsorption kinetic and equilibrium studies for methylene blue dye by partially hydrolyzed polyacrylamide/cellulose nanocrystal nanocomposite hydrogels, Chem. Eng. J., **251**, 17–24 (2014).

3. **Wu, S., Zhao, X., Li, Y., Du, Q., Sun, J., Wang, Y., Wang, X., Xia, Y., Wang, Z., Xia, L.**: Adsorption properties of doxorubicin hydrochloride onto graphene oxide: Equilibrium, kinetic and thermodynamic studies, Materials (Basel)., **6**, 2026–2042 (2013).

4. **Evans, C., Morimitsu, Y., Hisadome, T., Inomoto, F., Yoshida, M., Takei, T.**: Optimized hydrophobically modified chitosan cryogels for strength and drug delivery systems, J. Biosci. Bioeng., **132**, 81–87 (2021).

5. **Evans, C., Morimitsu, Y., Nishi, R., Yoshida, M., Takei, T.**: Novel method to fabricate hydrophobically modified agarose cryogels, J. Biosci. Bioeng., **In Press**,

https://doi.org/10.1016/j.jbiosc.2021.12.009 (2021).

6. **Oladipo, A. A., Gazi, M., Saber-Samandari, S.**: Adsorption of anthraquinone dye onto eco-friendly semi-IPN biocomposite hydrogel: Equilibrium isotherms, kinetic studies, and optimization, J. Taiwan Inst. Chem. Eng., **45**, 653–664 (2014).

7. **Liu, Y., Hu, X.**: Kinetics and thermodynamics of efficient phosphorus removal by a composite fiber, Appl. Sci., **9** (2019).

8. **Dada, A. O., Olalekan, A. P., Olatunya, A. M., Dada**: Langmuir, Freundlich, Temkin and Dubinin-Radushkevich isotherms studies of equilibrium sorption of Zn 2+ unto phosphoric acid modified rice husk, IOSR J. Appl. Chem. (IOSR-JAC, **3**, 38–45 (2012).

9. **Fosso-Kankeu, E., Mittal, H., Waanders, F., Ray, S. S.**: Thermodynamic properties and adsorption behavior of hydrogel nanocomposites for cadmium removal from mine effluents, J. Ind. Eng. Chem., **48**, 151–161 (2017).

10. **Al-Ghouti, M. A., Da'ana, D. A.**: Guidelines for the use and interpretation of adsorption isotherm models: A review, J. Hazard. Mater., **393**, 122383 (2020).

11. **Almukhtar, J. G. J., Karam, F. F.**: Kinetic and thermodynamic studies for mebeverine hydrochloride adsorption from aqueous solution using prepared chitosan polymer in delivery drug system, J. Phys. Conf. Ser., **1664** (2020).

12. **Ullah, S., Bustam, M. A., Assiri, M. A., Al-Sehemi, A. G., Gonfa, G., Mukhtar, A., Abdul Kareem, F. A., Ayoub, M., Saqib, S., Mellon, N. B.**: Synthesis and

characterization of mesoporous MOF UMCM-1 for CO2/CH4 adsorption; an experimental, isotherm modeling and thermodynamic study, Microporous Mesoporous Mater., **294**, 109844 (2020).

13. **Milonjić, S. K.**: A consideration of the correct calculation of thermodynamic parameters of adsorption, J. Serbian Chem. Soc., **72**, 1363–1367 (2007).

14. **Vieira, T., Artifon, S. E. S., Cesco, C. T., Vilela, P. B., Becegato, V. A., Paulino, A. T.**: Chitosan-based hydrogels for the sorption of metals and dyes in water: isothermal, kinetic, and thermodynamic evaluations, Colloid Polym. Sci., **299**, 649–662 (2020).

15. **Inyinbor, A. A., Adekola, F. A., Olatunji, G. A.**: Kinetics, isotherms and thermodynamic modeling of liquid phase adsorption of Rhodamine B dye onto Raphia hookerie fruit epicarp, Water Resour. Ind., **15**, 14–27 (2016).

16. **Shahwan, T.**: Lagergren equation: Can maximum loading of sorption replace equilibrium loading?, Chem. Eng. Res. Des., **96**, 172–176 (2015).

Chapter 5 *Conclusion*

5-1 CONCLUSION

A review of the current literature surrounding hydrophobically modified polymers showed that a lot of research leaned towards the use of synthetic polymers that were copolymerized, grafted, or chemical crosslinked. Research into hydrophobically modifying natural polymers and using hydrophobic modification to physically crosslink gels was limited. As such, this research aimed to increase the knowledge of hydrophobically modified polysaccharide polymers. To do this, the following questions were asked:

1. Can polysaccharide polymers be hydrophobically modified?

2. If so, can these hydrophobically modified polysaccharide polymers be fabricated into hydrogels?

3. If successful fabrication of hydrogels occurs, what are the characteristics of the created hydrogels?

4. If successful fabrication of hydrogels occurs, what are the chemical engineering processes the gels undergo during the adsorption process of hydrophobic liquids?

5. Based on these limitations and delimitations what areas of use would the gel/gels have in the biomedical field?

In Chapter 2, we fabricated HMC polymers which we then developed into cryogels. Through testing on the produced cryogels, we were able to determine that the alkyl chain

lengths and the substitution degree influenced the characteristics of the cryogel. We were able to identify that the C8/7% cryogel had the highest mechanical performance and that the C12/15% was optimal for the adsorption and release of hydrophobic dyes. We identified that HMC cryogels had the potential to be biomaterials, perhaps carriers of hydrophobic drugs.

In Chapter 3, we fabricated HMA polymers and developed a novel method of producing HMA cryogels. Testing showed that the mechanical properties didn't differ from the more traditional methods of unmodified agarose fabrication (for example, hydrogels produced using water). We determined that the cytotoxicity of the HMA10 cryogel was extremely low though cellular adhesion was higher when compared to traditionally fabricated agarose hydrogels. HMA10 also had more control over the adsorption and diffusion of hydrophobic dye compared to unmodified agarose cryogels. We identified that HMA cryogels had the potential to be used as biomaterials, again perhaps as carriers of hydrophobic drugs.

In Chapter 4, we determined the isotherms, kinetics, and thermodynamics of HMC and HMA cryogels. By doing so, we attempted to better understand the chemical processes that HMA and HMC cryogels undergo when adsorbing hydrophobic dyes. It was discovered that Langmuir's isotherm model was better suited to HMC cryogels while Freundlich's isotherm was better suited to HMA cryogels. Both HMC and HMA indicated that the adsorption process was spontaneous, and that adsorption happened very quickly and was temperature dependent. Finally, both HMC and HMA cryogels matched better to the pseudo second order than the pseudo-first order.

Based on the research described in this dissertation we have shown that polysaccharide polymers can be hydrophobically modified (chitosan and agarose) and that new methods of modification have been created to do so. We have shown that hydrophobically modified polysaccharide polymers can be fabricated into cryogels through hydrophobic physical crosslinking and that the characteristics of the fabricated cryogels have been discovered. We have shown that the chemical engineering processes the gels undergo during the adsorption process of hydrophobic liquids has been recognized and finally, we have discussed, based on the identification of characteristics, the limitations, and delimitations of the fabrication process and the thermodynamic processes, the fabricated gels have the potential to be used as biomaterials, particularly as drug delivery systems.

5-2 FUTURE RESEARCH

In the future, we would like to determine an exact biomedical application for HMA and HMC cryogels. We would like to experiment on using HMA cryogels as transdermal carriers of a specific hydrophobic drug and on HMC cryogels as either transdermal carriers or mucosal carriers of specific hydrophobic drugs.

Acknowledgements

This work was carried out in the Yoshida-Takei Laboratory, Department of Chemical Engineering, Faculty of Science and Engineering, Kagoshima University.

This research would not have been possible without the help of many people. I would like to take this opportunity to thank them for their support.

First and foremost, I am extremely grateful to my supervisor Professor Takayuki Takei for the opportunity to take part in this research. His knowledge and experience on the subject matter has helped guide me through my academic research and his insightful critique and encouragement of my methods and conclusions has inspired my growth as a researcher. I am also grateful to Professor Susumu Nii and Professor Masahiro Yoshida for giving up their valuable time to review this dissertation and for their invaluable comments and suggestions.

I would like to recognize the Yoshida-Takei Laboratory group members for their helpful assistance and practical contributions throughout my research. A special thank you goes to Mr. Yuto Morrimitsu and Miss. Rikako Nishi for their guidance and instruction on experimental research.

I would like to acknowledge the Rotary Yoneyama Scholarship group (in particular, my host club Kagoshima West Rotary Club) who in my final year accepted me as a scholarship recipient, and the Japan Society for the Promotion of Science for their financial aid.

Finally, to my parents, brother, and friends (especially Francisco Perez-Smith), thank you for being so unconditionally supportive and encouraging during my research.